Supporting Online Material

Pulsatile stimulation determines timing and specificity of NF-kappa B-dependent transcription

**L. Ashall, *C.A. Horton, *D.E. Nelson, *P. Paszek, C.V. Harper, K. Sillitoe, S. Ryan, D.G. Spiller, J.F. Unit, D.S. Broomhead, D.B. Kel, D.A. Rand, V. Sée, and M.R.H. White.*

Correspondence to Professor M. White: mwhite@liv.ac.uk, Tel. +44(0)151-7954424, Fax. 44-(0)151-7954404

Index:

1. Materials and Methods
2. Supporting data
   - Section A: Further data on oscillatory kinetics
   - Section B: Synchronisation of NF-κB signalling and system reset
   - Section C: Experimental and computational analysis of IκBε feedback
   - Section D: Function of NF-κB oscillation frequency
3. Mathematical modeling
   - Section A: Deterministic 2-feedback NF-κB model
   - Section B: Stochastic 3-feedback NF-κB model
   - Section C: Model equations
4. Author contributions
5. References

1. Materials and Methods

Materials: Human and mouse recombinant TNFα was supplied by Calbiochem (UK). Tissue culture medium was supplied by Invitrogen (UK) and Fetal Calf Serum (FCS) was from Harlan Seralab (UK). All other chemicals were supplied by Sigma (UK) unless stated otherwise.

Plasmids: All plasmids were propagated using *E.coli* DH5α and purified using Qiagen Maxiprep kits (Qiagen, UK). RelA-dsRedxp contains the optimized dsRed-Express fluorescent protein (Clontech, CA, USA) fused to the C-terminus of RelA.

Cell culture: MEF cells (received from Ron Hay, Dundee) were grown in Dulbecco's Minimal Essential Medium (41966, Gibco) plus 10% FCS. HeLa and SK-N-AS cells were grown as described in (*1*). To generate stable cell lines, SK-N-AS cells were stably transfected with RelA-dsRedxp using Fugene 6 and maintained in MEM supplemented with 10% FCS and 1% NEAA. Clones were obtained (using ring cloning) and recloned under G418 (500 μg/ml; GIBCO-BRL, Paisley, UK) selection. Clones were assessed for the expression of RelA-dsRedxp and responses to TNFα. The selected clone had low but detectable expression of fluorescent protein and G418 did not influence results.
For confocal fluorescence microscopy, MEF or SK-N-AS cells were plated on 35 mm glass-bottom dishes (Iwaki, Japan) at $1x10^5$ cells per dish in 3 ml medium. 24 h post-plating, the cells were transfected with the appropriate plasmid(s) using Fugene 6 (Boehringer Mannheim/Roche, Germany) in accordance with the manufacturer's recommendations. The optimised ratio of DNA:Fugene 6 used for transfection of MEF or SK-N-AS cells was 2 μg DNA with 4 μl Fugene 6 and 0.8 μg DNA with 1.2 μl Fugene 6 respectively. For siRNA confocal microscopy, SK-N-AS cells were plated 35 mm glass-bottom dishes (Iwaki, Japan) at 3.75×10^5 cells per dish in 2 ml medium. Cells were transfected the same day with 87.5 pmol of either *Silencer*® Pre-designed IκBε (ID:115539) siRNA, *Silencer*® Negative control #1 siRNA (Ambion), Cyclophilin A siRNA (Dharmacon) and 1 μg of expression vector using Lipofectamine 2000 (Invitrogen) and Opti-MEM (Gibco) in accordance with the manufacturer's recommendations. 24 h post-plating, the medium was removed and replaced with fresh medium. For ChIP assays, SK-N-AS cells were plated on 100 mm tissue culture dishes (Iwaki, Japan) at $4.5x10^6$ cells per dish in 10 ml medium. For Western blotting, semi-quantitative and quantitative RT-PCR, HeLa and SK-N-AS cells were plated on 60 mm tissue culture dishes (Iwaki, Japan) at $5x10^5$ and $1x10^6$ cells respectively per dish in 5 ml medium.

Treatment of cells with TNFα: TNFα was used in all experiments at 10ng/ml. For confocal fluorescence microscopy, the cells were treated with TNFα 24 h post-transfection and 48 h post-transfection for siRNA experiments. For western blotting and RT-PCR experiments the cells were treated with TNFα 24 h post-plating. For ChIP assays the cells were treated with TNFα 48 h post-plating by replacing one tenth of the media volume with media containing 100 ng/ml TNFα. For experiments using continual TNFα stimulation the TNFα-containing medium was left on the cells for the duration of the experiment. For TNFα pulse experiments, the cells were stimulated with TNFα for 5-

minutes and then washed 3 times with fresh medium at 37°C. The cells were imaged either immediately after treatment or incubated (at 37°C, 5% CO_2) for the indicated duration prior to cell lysis or fixation.

Fluoresence microscopy: Confocal microscopy was carried out as described in (*1*) using either 40x or 63x objectives. Multiple field time lapse imaging with autofocus was performed using the macro described in (*2*). CellTracker version 0.6 (DTI Beacon project, H. Shen, University of Manchester (*3*)) was used for data extraction. For RelA fusion proteins, mean fluorescence intensities were calculated for each time point for both nuclei and cytoplasm then nuclear:cytoplasmic (N:C) fluorescence intensity ratios were determined. For all experiments the imaging duration was determined by the degree to which cells were likely to move out of the field during the experiment (this was a particular issue that limited the number of MEF cells that could be analyzed in a particular time due to the greater extent of cell movement).

ChIP assays: ChIP assays were carried out based on the protocol described by Upstate Biotechnology with some alterations to the manufacturer's guidelines.
Formaldehyde cross-linking After the indicated times of TNFα stimulation, formaldehyde was added to each plate at a final concentration of 1% and incubated at room temperature for 15 min. Plates were kept on ice and the medium was aspirated and cells washed twice with PBS supplemented with protease inhibitors (1 mM phenyl methyl sulphonyl fluoride (PMSF), 1x mammalian protease inhibitor cocktail). Cells were scraped into 500 µl of PBS with protease inhibitors, centrifuged (4 min, 2000 rpm at 4°C) and the pellet resuspended in 200 µl SDS lysis buffer (1% (w/v) SDS, 10 mM EDTA, 50 mM Tris-HCl pH 8) with protease inhibitors and incubated on ice for 10 min.
Sonication Cells were sonicated on ice using a Sonics Vibra cell (VCX 130 PB) sonicator at 30 % amplitude for 5 x 10 s pulses. Samples were left on ice at least 1 min between each pulse.
Immunoprecipitation Following shearing, samples were centrifuged (10 min, 13000 rpm at 4 °C). The supernatant was collected and 1.8 ml ChIP dilution buffer (0.01% (w/v) SDS, 1.1% (v/v) Triton X-100, 1.2 mM EDTA, 16.7 mM Tris-HCl pH 8, 167 mM NaCl) with protease inhibitors was added. 200 µl was removed for the input material and frozen at -20 °C. Salmon sperm DNA/protein A agarose (Upstate Biotechnology) (75 µl) was added to each sample and incubated for 30 min at 4 °C with rotation to clear the DNA. The agarose beads were pelleted by centrifugation (60 sec, 4000 rpm at 4 °C) and the supernatant collected. 5 µg Antibody either Anti-RelA, Anti-IgG, Anti-RNA polymerase II (Upstate Biotechnology), was added to each sample and incubated overnight at 4 °C with rotation. Salmon sperm DNA/protein A agarose (60 µl) was added to each sample and incubated for 1 h at 4 °C with rotation. The agarose beads were pelleted by centrifugation (60 sec, 4000 rpm at 4 °C) and washed with low salt immune complex wash buffer (0.1% SDS, 1% Triton X-100, 2 mM EDTA, 20 mM Tris-HCl pH 8, 150 mM NaCl) and incubated for 3-5 min at 4 °C with rotation. This was repeated with high salt immune complex wash buffer (0.1% SDS, 1% Triton X-100, 2 mM EDTA, 20 mM Tris-HCl pH 8, 500 mM NaCl), followed by lithium chloride immune complex wash buffer (0.25 M LiCl, 1% Nonidet P40, 1% deoxycholate, 1 mM EDTA, 10 mM Tris-HCl pH 8), and two washes with TE (10 mM Tris-HCl pH 8, 1 mM EDTA).

Extracting DNA The protein/DNA complex was eluted from the beads by adding 250 µl of elution buffer (0.1% SDS, 0.1 M $NaHCO_3$), vortexing briefly and incubating at room temperature with rotation for 30 min. The beads were centrifuged (60 sec, 4000 rpm at room temperature), the supernatant collected and added to a further 250 µl of elution buffer. Elution buffer (300 µl) was also added to the input material samples, to get the same 500 µl volume as the immunoprecipitated samples. Samples were adjusted to 0.2 M NaCl and incubated at 65 °C for 4 h to reverse the cross links. A further incubation step was carried out for 1 h at 45 °C in the presence of 9 mM EDTA, 36.2 mM Tris-HCl, pH 6.5 and 2 µl of 10 mg/ml Proteinase K to each sample. The DNA was purified using the QIAquick PCR Purification kit (Qiagen) according to manufacturer's instructions and eluted into a final volume of 30 µl.

PCR conditions For PCR amplification, 4 µl of immunoprecipitated DNA or 2 µl of input DNA was used per reaction combined with a mastermix consisting of 1x NH_4 reaction buffer (Bioline), 80 µM dNTPs (Bioline), 2 mM $MgCl_2$, 20 pmol of each primer, 1 u Biotaq DNA polymerase (Bioline) made up to a total reaction volume of 25 µl with dH_2O. The PCR reaction was performed using a Px2 Thermo Cycler (Thermo-Electron Corporation, USA) with the following cycle conditions: initial denaturation at 94 °C for 2 min, denaturation at 94 °C for 30 sec, annealing at 58 °C for 30 sec, elongation at 72 °C for 1 min for 36 cycles and hold at 72 °C for 5 min. The primer sequences used: IκBα (NM_020529) left TCAAATCGATCGTGGGAAA, right GGACTGCTGTGGGCTCTG amplifying 360 bp and IκBε (NM_004556) left GGGACTAAGATTGGGGCTGT, right CCTATCCCCTGCCCATTTAT amplifying 395 bp. PCR products were combined with orangeG and were resolved by 1.2 % agarose gel electrophoresis containing 0.5 µg/ml ethidium bromide against 1 kb Plus DNA ladder (Invitrogen, UK). Products were visualised under UV illumination and imaged using the G:box gel documentation and analysis system (Syngene, UK) and were analysed by AQM Advance 6.0 software (Kinetic Imaging, UK).

RT-PCR

mRNA extraction The RNeasy Mini Kit (Qiagen, Germany) was used to extract mRNA from the cells following manufacturer's instructions. The mRNA concentration and purity was quantified using a UV-1601 UV-Visible spectrophotometer (Shimadzu, Japan). The absorbance was measured at 260 and 280 nm. All mRNA were of sufficient purity with a A_{260}/A_{280} ratio between 1.9-2.1 used in the reverse transcriptase reaction.

Production of cDNA for semi-quantitative PCR For each sample, 2 µg of mRNA was used in a total volume of 11 µl (diluted in RNase free water) combined with 1x M-MLV buffer (Promega, USA), 2.5 mM dNTPs and 1 µl of random primers (Promega, USA) in 0.5 ml PCR tubes and incubated at 70°C for 10 min using a Px2 Thermo Cycler (Thermo-Electron Corporation, USA). The samples were then returned to ice and 20 u of recombinant RNasin© Ribonuclease Inhibitor (Promega, USA) and 200 U of M-MLV reverse transcriptase (Promega, USA) were added. Samples were then incubated at 25°C for 10 min, 42°C for 60 min, and then 90°C for 2 min in the PCR machine. The resultant cDNA was diluted with 25 µl of RNase free water and stored at -20°C.

Amplification of cDNA for semi-quantitative PCR For PCR amplification 5 µl of each cDNA sample was used per reaction combined with a mastermix consisting of 1x NH_4 reaction buffer (Bioline), 80 µM dNTPs (Bioline), 2mM $MgCl_2$, 20 pmol of each primer

(A20 left CACGCTCAAGGAAACAGACA, right CATGGGTGTGTCTGTGGAAG, IκBα left GGGCTGAAGAAGGAGCGGC, right TCCATGGTCAGTGCCTTTTCTTCA, IκBε left GCCTGGTACAGTTCCTGCTC, right TCATCAAAGGGCAAAAGGAC, p100 left GAACAGCCTTGCATCTAGCC, right TCCGAGTCGCTATCAGAGGT, RANTES left TGTACTCCCGAACCCATTTC, right CGCTGTCATCCTCATTGCTA, cyclophilin A left GACCCAACACAAATGGTTCC, right TCGAGTTGTCCACAGTCAGC) and 1 U Biotaq DNA polymerase (Bioline), made up to a final volume with dH_2O to 25 µl. The PCR reaction was performed using a Px2 Thermo Cycler (Thermo-Electron Corporation, USA) with cycling parameters as follows: initial denaturation at 95 °C for 2 min, 94 °C for 30 sec, 58 °C for 30 sec and 60 °C for 30 sec, hold at 72 °C for 5 min. Products were combined with orangeG and were resolved by 1.5 % agarose gel electrophoresis containing 0.5 µg/ml ethidium bromide against 1 kb Plus DNA ladder (Invitrogen, UK).

Production of cDNA for qPCR The QuantiTect reverse transcription kit (Qiagen, Germany) was used for production of cDNA. For each sample, 1 µg of mRNA was used. Manufacturer's protocol was followed except the incubation time at 42 ˚C was extended from 15 min to 30 min. The cDNA was diluted 1:1 with RNase free water.

Amplification of cDNA for qPCR In each reaction 1 µl of cDNA was incubated with 300 nM of each primer: IκBα left TGGTGTCCTTGGGTGCTGAT right GGCAGTCCGGCCATTACA, IκBε left GGACCCTGAAACACCGTTGT right CCCCAGTGGCTCAGTTCAGA, MCP-1 left CAAGCAGAAGTGGGTTCAGGAT right TCTTCGGAGTTTGGGTTTGC, RANTES left GTCGTCTTTGTCACCCGAAAG right TCCCGAACCCATTTCTTCTCT, cyclophilin A left GCTTTGGGTCCAGGAATG right GTTGTCCACAGTCAGCAATGGT, 1 x Power SYBR Green PCR mastermix (Applied Biosystems) with RNase free water added to a total volume of 20 µl. The cycling parameters were as follows: initial denaturation at 95 °C for 10 min, 95 °C for 15 sec, 58 °C for 30 sec and 60 °C for 30 sec carried out on an ABI7500 Fast thermocycler for 45 cycles with a dissociation curve completed at the end of each run. The efficiency of the primers was tested, which gave a slope value of around -3.32 and R^2 value of 0.99. Relative quantification was used to calculate the fold difference based on the threshold cycle (CT) value for each PCR reaction using $2^{-\Delta\Delta CT}$ method. The target gene was normalised to the reference gene cyclophilinA, with time 0 min used as the calibrator.

Western blotting: Whole cell lysates were prepared at the indicated times after stimulation. Proteins were separated by polyacrylamide gel (10%) electrophoresis then transferred to nitrocellulose membranes. Membranes were probed using the following antibodies: anti-IκBα (#9242, Cell Signaling, MA, USA), anti-phospho-IκBα (Ser 32) (#9241, Cell Signaling, MA, USA), anti-RelA (#3034, Cell Signaling, MA, USA) and anti-phospho-RelA (Ser 536) (#3031, Cell Signaling, MA, USA), anti-IκBε (#7156, Santa Cruz Biotechnology, USA) and anti-cyclophilin A (#07-313, Upstate Biotechnology, USA). Band intensity was quantified using a BioRad GS-710 Densitometer and Quantity One software (Version 4.5.0).

2. Supporting data

Section A: Further data on oscillatory kinetics.
It was hypothesised that chromatin immunoprecipitation (ChIP) assays were the most likely method to detect oscillations in an untransfected cell population, as DNA binding of the transcription factor to target gene promoters was the first consequence of nuclear entry. We observe cycles of binding of RelA to the IκBα and IκBε promoters in SK-N-AS cells, (Fig. S1A & C, see also Fig. S12A). The timing of the observed DNA binding cycles closely matched that of single cell fluorescent protein translocation. In contrast, only a single peak of DNA binding was observed following a single 5-minute pulse of TNFα stimulation (Fig. S1B & D). These data support the view (*4-7*) that oscillations in RelA localization and DNA binding occur in single wild-type (transfected or untransfected) cells in response to TNFα, in a range of cell types.

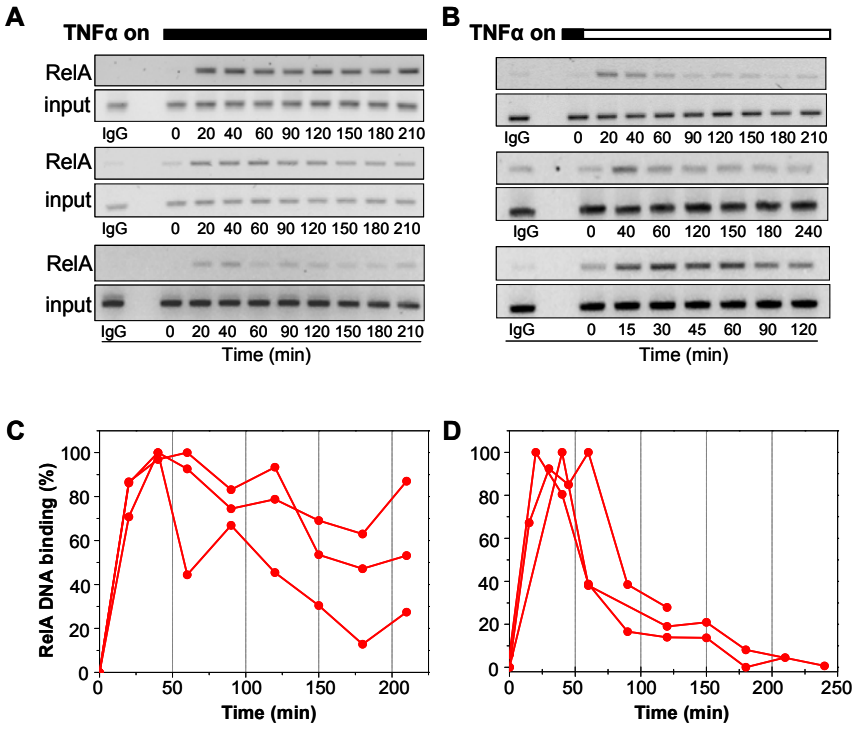

Fig. S1: ChIP analysis of RelA DNA binding. (A & B) RelA DNA binding levels at the IκBα promoter in SK-N-AS cells after (A) continuous TNFα and (B) a 5-minute TNFα pulse. (C & D) Densitometric analysis of data from the triplicate experiments shown in A & B, with binding levels normalised to highest intensity.

The average cell population is displayed in RelA-dsRedxp stably transfected SK-N-AS cells and in transiently transfected MEFs. Both showed a single peak of NF-κB nuclear localization (Fig. S2A & B). These average data masked the single cell N:C oscillations observed (Fig. 1A, C & E).

RelA-dsRedxp stably transfected SK-N-AS cells oscillated with a longer period of ~100 min (Fig. S2C) compared to transiently transfected MEF cells that oscillated with a period of typically ~80 min (Fig. S2D). Interestingly in the stable SK-N-AS cells, the timing between the first and second translocation of RelA-dsRedxp was greater than the timing between successive peaks. This might be explained through the observation that some cells displayed an initial longer period of RelA-dsRedxp nuclear localization (Fig. 1A).

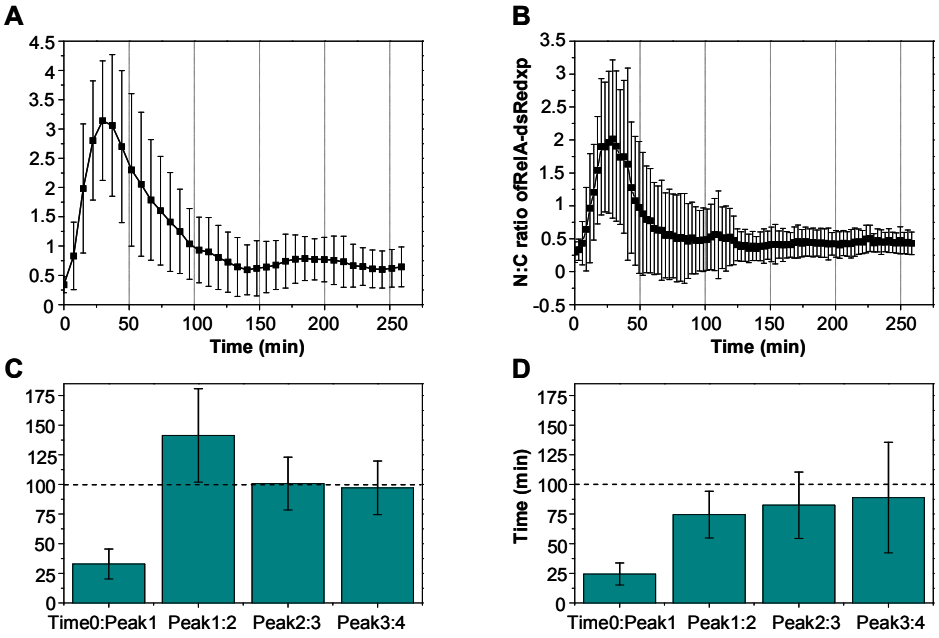

Fig. S2: Analysis of RelA oscillations. *(A & B) Time course of cell population average (±SD) of N:C localisation of RelA-dsRedxp for (A) SK-N-AS cells (n= 34) stably transfected and (B) MEF cells (n=25) transiently transfected after continuous 10 ng/ml TNFα stimulation. (C & D) Average timing between successive peaks (±SD) of translocations of RelA-dsRedxp for (C) SK-N-AS cells stably transfected and (D) MEF cells transiently transfected after continuous 10 ng/ml TNFα stimulation.*

Section B: Synchronisation of NF-κB signalling and system reset.
About 100%, 95% and 80% of cells analysed showed at least 2 of a possible 3 translocations for 200-, 100- and 60-minute TNFα pulses respectively (Fig. S3). These pulses gave synchronous cell responses across the population (Fig. S4) in contrast to the asynchrony observed after continuous TNFα stimulation (*1*).

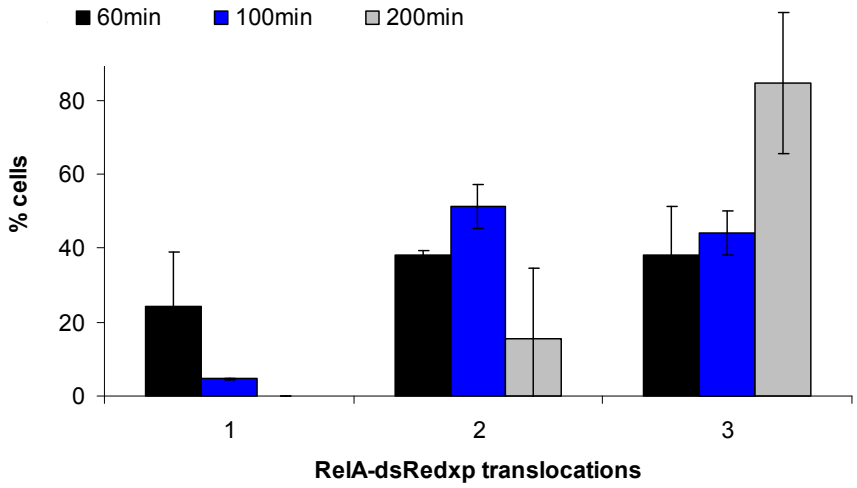

Fig. S3: Percentage of SK-N-AS cells responding to 3 x 5-minute TNFα pulses. *SK-N-AS cells transiently transfected with RelA-dsRedxp were stimulated with TNFα for 5-minutes at either 60- (n=26), 100- (n= 43) or 200-minute (n= 26) intervals. Shown are percentages of cells exhibiting 1, 2 or 3 N:C translocations.*

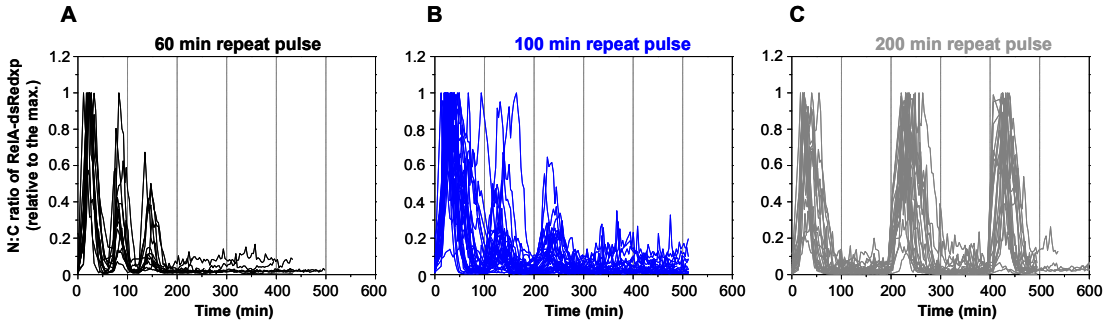

Fig. S4: Analysis of RelA-dsRedxp translocations in SK-N-AS cells pulsed with TNFα at intervals of 60- ,100-, or 200- minutes. *SK-N-AS cells transiently transfected with RelA-dsRedxp were stimulated with TNFα for 5- minutes at either (A) 60- (n= 12), (B) 100- (n= 34) or (C) 200- (n= 22) minute intervals. Immediately after the TNFα was added for the first stimulation, the cells were imaged every 3 min by confocal laser scanning microscopy. Mean nuclear and cytoplasmic RelA-dsRedxp fluorescence was quantified and plotted as average N:C fluorescence normalized to the amplitude of peak 1 vs. time. Each line represents a single cell.*

Western blot analysis of SK-N-AS cells stimulated with a 5-minute TNFα pulse at 60-minute intervals showed an increase in phospho-IκBα and phospho-RelA levels after both the first and second pulse, which correlated with a decrease in total IκBα levels (Fig. S5A and Fig. S6). A third increase in phospho-IκBα levels could also be detected by 120 min. IκBα was not completely degraded after the second TNFα pulse, which correlates with the damping of RelA-dsRedxp nucleo-cytoplasmic oscillations (Fig. 2A). When cells were pulsed with TNFα at 100-minute intervals (Fig. S5B and Fig. S6) similar patterns of phosphorylation of IκBα and RelA and degradation of IκBα were observed compared to those seen following pulses at 60-minute intervals.

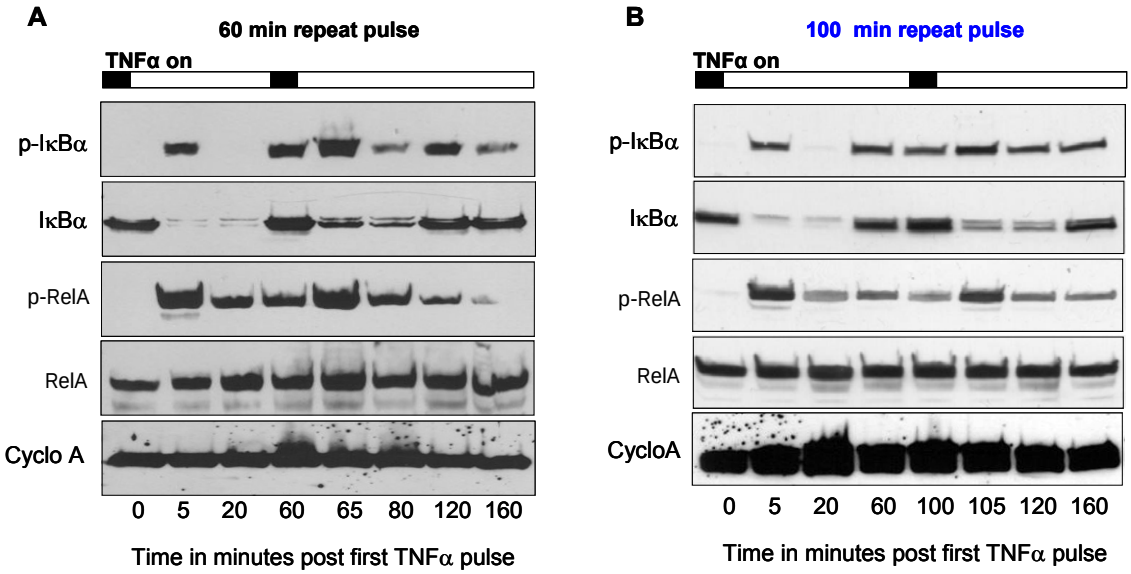

Fig. S5: Western blot analysis of RelA and IκBα phosphorylation and IκBα degradation in SK-N-AS cells pulsed with TNFα at intervals of 60- or 100-minutes. *SK-N-AS cells were stimulated twice with TNFα for 5-minutes at either (A) 60- or (B) 100- minute intervals. Cells were lysed at the indicated times and analyzed for serine 32 phospho-IκBα (p-IκBα), total IκBα (IκBα), serine 536 phospho-RelA (p-RelA), total RelA and cyclophilin A (Cyclo A) protein levels.*

In contrast to SK-N-AS cells pulsed at 60- and 100-minute intervals, pulsing at 200-minutes allowed for efficient IκBα degradation both after the first and second TNFα pulse (Fig. S6). This correlated with the fact that RelA-dsRedxp translocation amplitudes were not damped as observed through imaging experiments (Fig. 2A), providing further evidence that within the 200-minute period, the system had reset.

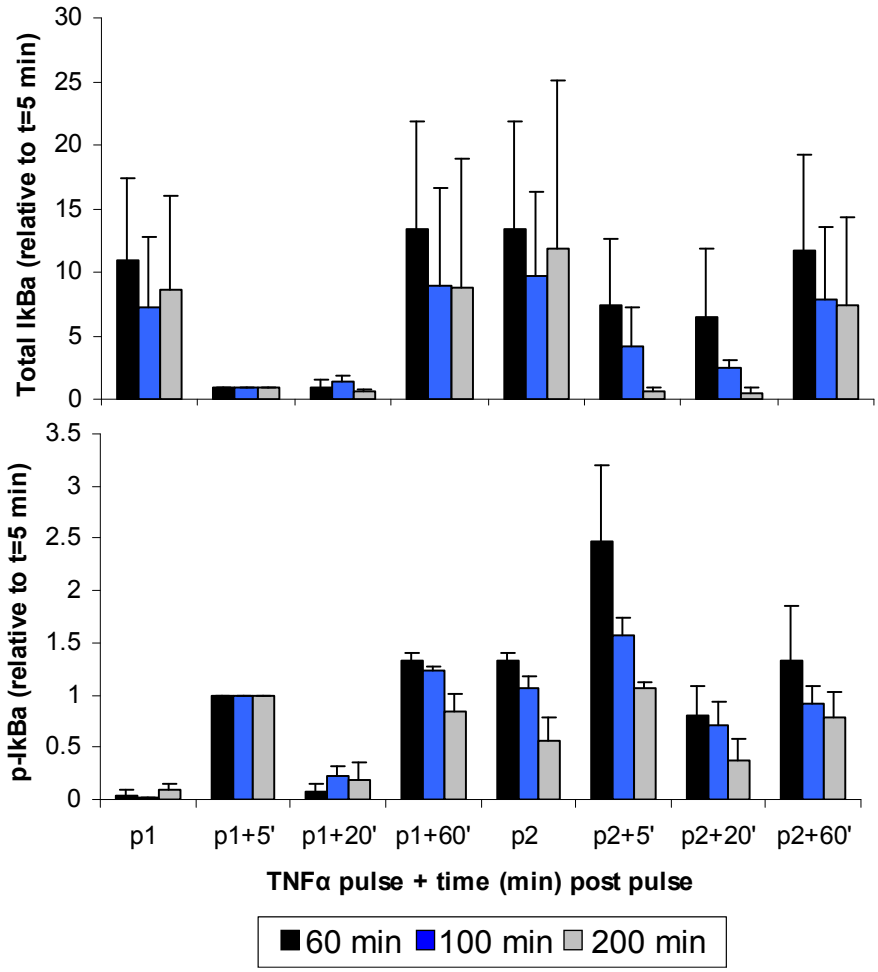

Fig. S6: Analysis of western blot data in SK-N-AS cells pulsed with TNFα at intervals of 60-, 100- or 200-minutes. *Densitometry analysis for western blot data (Fig. 2C and Fig. S5) for the total IκBα and Ser32 phospho-IκBα (p-IκBα) levels in SK-N-AS cells stimulated with a 5-minute TNFα pulse at 60-, 100- and 200-minute intervals (+SD). Analysis based on 3 replicates for each stimulation protocol normalized relative to t= 5-minutes. Shown are amplitudes at the times past the respective TNFα pulse (p1, p2) for each simulation protocol, respectively.*

The existing models were tested for their ability to predict the system to reset (given repetitively pulsed TNFα stimulation) (Fig. 2A), and the continuous (*1*) and single TNFα pulsing of varying durations (Fig. S7). In Fig. S8 we show that the existing IKK network structure (*8*) failed to simultaneously fit repeat pulsing and continuous TNFα stimulation because of the conflict between high IKK activity required for the former and low IKK activity for the latter. Inability of the existing model to fit was confirmed by scanning all model parameters both individually (Fig. S9A) and in pairs (see Fig. S9B for an example of dual parameter scan). Parameter scans performed in Fig. S10 showed robustness of the proposed structure (Fig. 2G) to significant variations in model parameters. It also allowed identification of groups of parameters that were sensitive to all simulation conditions (e.g., *ki*, *kc2a*, *c1a and c3a*), sensitive to continuous TNFα but not repeat pulsing stimulation (e.g., *kp*, *kbA20*, c1 and *c3*), or sensitive to TNFα repeat pulsing but not continuous stimulation (*ka*).

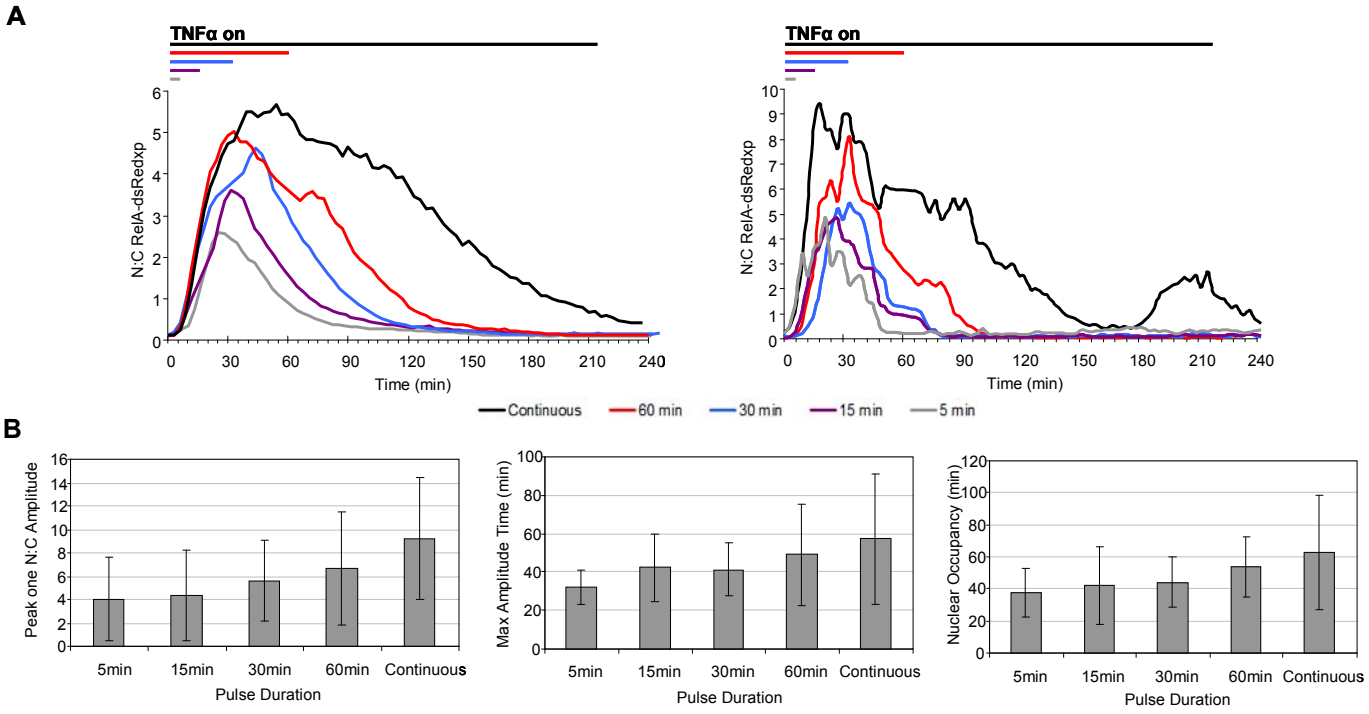

Fig. S7: Effect of increasing the duration of TNFα pulse on the characteristics of the initial NF-κB translocation. *SK-N-AS cells were co-transfected with RelA-dsRedxp and pEGFP-N1. 24 h post-transfection, cells were pulsed for the indicated times or continuously stimulated. Data plotted as average N:C fluorescence intensity at each time-point (A, left), or single cell N:C (A, right) over time. Individual cells (A, right) selected based on nearest to mean peak N:C amplitude for each pulse duration condition. (B) Quantitative analysis of single cell peak characteristics from N:C RelA-dsRedxp time-series. Shown from left to right: Peak amplitude, peak time and nuclear occupancy time (quantified as the peak width at half maximum amplitude), plotted as the average (+/-SD) (N ≥ 31 cells across ≥ 2 experiments).*

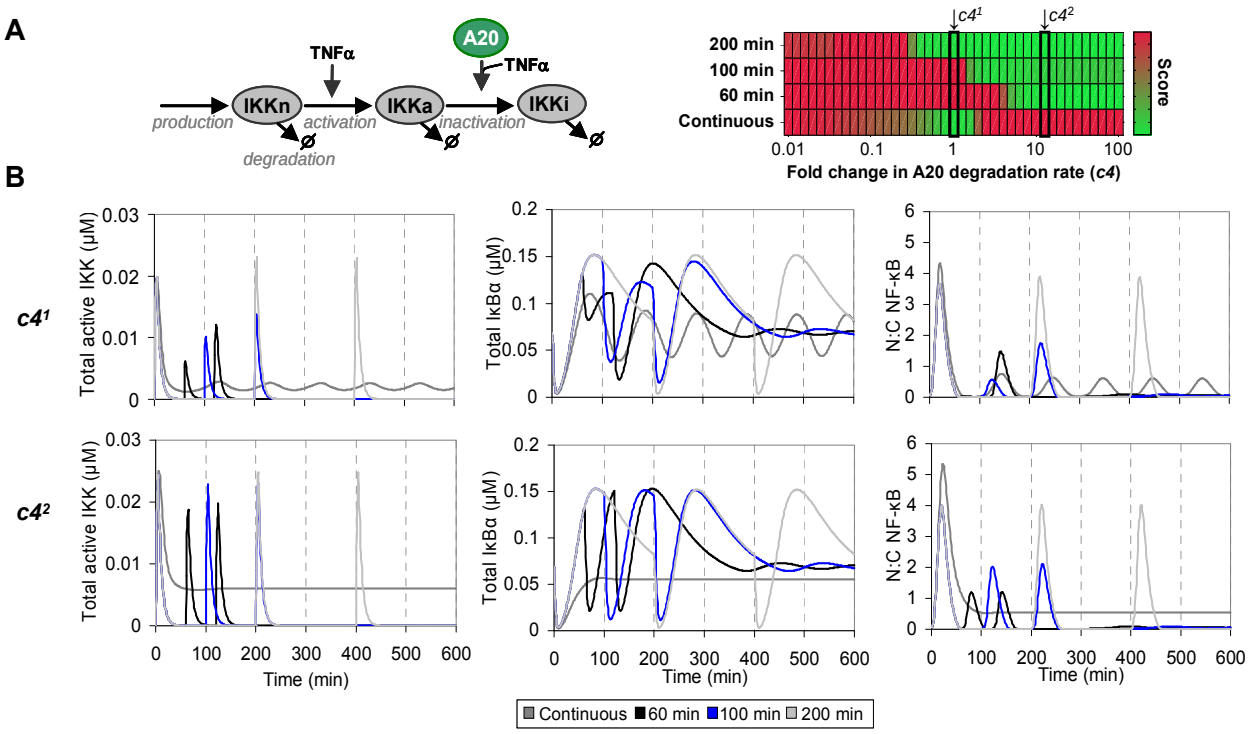

Fig. S8: Computational analysis of the existing IKK structure. (A) Ability of the existing IKK structure (left) combined with the Base Module (Table S1, Table S2 and Table S3) to simulate both the repeat pulsing and continuous TNFα stimulation conditions. The heat map (right) represents the score of a model fit (see scoring function section below) for a selected parameter scan. A20 degradation rate (c4) is varied on a logarithmic scale two orders of magnitude above/below a start value of *0.0009* s^{-1}. The goodness-of-fit score is represented on a scale from green (good) to red (poor) quantified by the distance of the simulation from the target (Table S5). Non-overlapping green regions indicate that the model cannot fit all conditions for the scanned range of parameter values. (B) Simulated time-series for two values of A20 degradation rate ($c4^1$=*0.0113* s^{-1} (top) and $c4^2$=*0.0009* s^{-1} (bottom)) selected from regions of good fit (as indicated by the arrows on the heat map in (A)). Nuclear to cytoplasmic ratios are displayed for NF-κB containing molecular species (right), as well as total cell IκBα (centre) and active IKK (left).

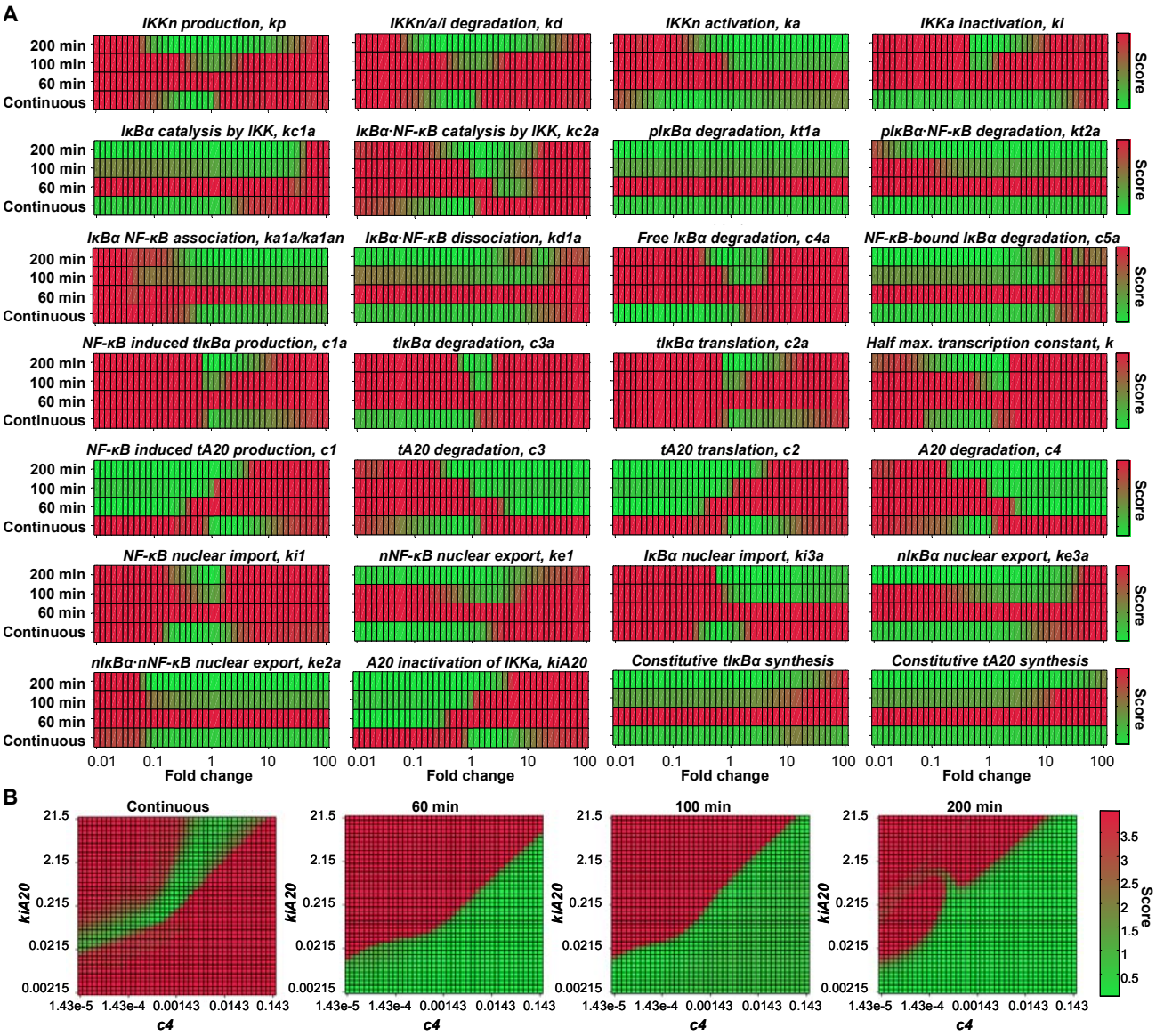

Fig. S9: Analysis of model parameters in the Base NF-κB model with the Existing IKK structure. *Heat maps represent the score (red-poor to green-good) of model fit (see scoring function section below) for the change in (A) a single or (B) two model parameters for four TNFα stimulation conditions as labeled. The starting values for parameter scans are summarized in Table S1, Table S2, and Table S3. Each parameter was varied on a logarithmic scale two orders of magnitude above/below start values, with all other parameters fixed. (A) In scans for kp, kd was scaled to conserve total IKK level, similarly when scanning kd, kp was scaled accordingly. In tIκBα and tA20 constitutive synthesis scans these parameter start values were $1\times10^{-9}s^{-1}$, in all other scans they were zero. (B) Dual parameter scans showing the dependence between A20 stability (c4) and inhibition (kiA20).*

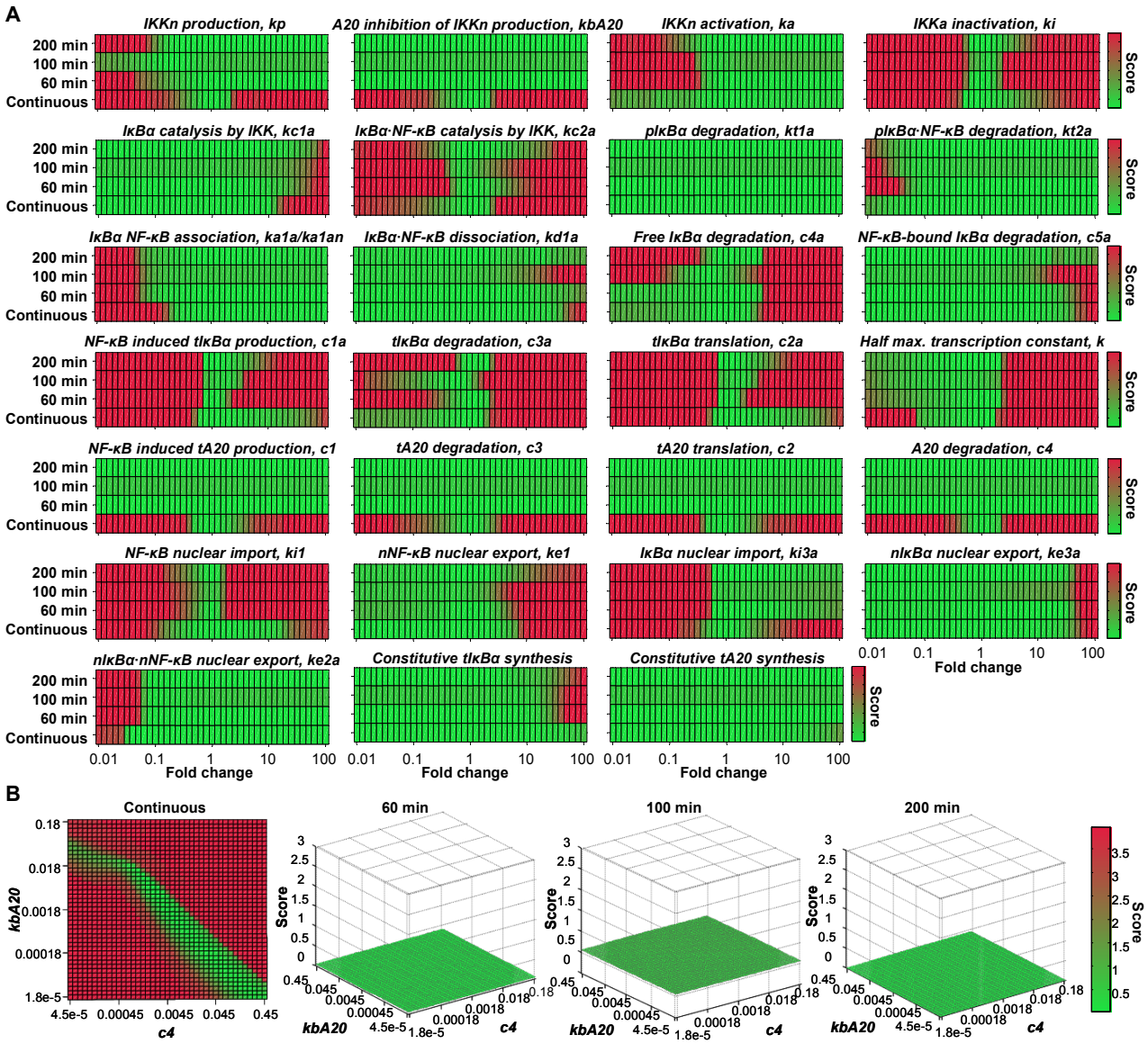

Fig. S10: Analysis of model parameters in the Base NF-κB model with the Proposed IKK structure. *Heat maps represent the score (red-poor to green-good) of model fit (see scoring function section below) for the change in (A) a single or (B) two model parameters for four TNFα stimulation conditions as labeled. The starting values for parameter scans are summarized in Table S1, Table S2, and Table S4. Each parameter was varied on a logarithmic scale two orders of magnitude above/below start values, with all other parameters fixed. (A) In tIκBα and tA20 constitutive synthesis scans these parameter start values were $1\times10^{-9}s^{-1}$, in all other scans they were zero. (B) Dual parameter scans showing the dependence between A20 stability (c4) and inhibition (kbA20) parameters. Pulsed conditions rely on early IKK activation kinetics and show little dependence on A20.*

Section C: Experimental and computational analysis of IκBε feedback loop.
In MEF cells, NF-κB signaling is controlled by two anti-phase feedback loops as NF-κB-mediated transcription of the IκBε gene was delayed relative to that of IκBα (*9*). A similar delay of 45-minutes in transcriptional regulation of IκBε in human SK-N-AS and HeLa cells was observed (Fig. S12B). The recovery of IκBε protein in the cytoplasm after initial rapid IKK-mediated degradation was further delayed with respect to that of the mRNA transcript level. While the IκBα protein was restored at about 60-minutes after TNFα stimulation (detected at 30-minutes), newly synthesized IκBε protein was restored at 2-hours in both SK-N-AS and HeLa cells (Fig. S11).

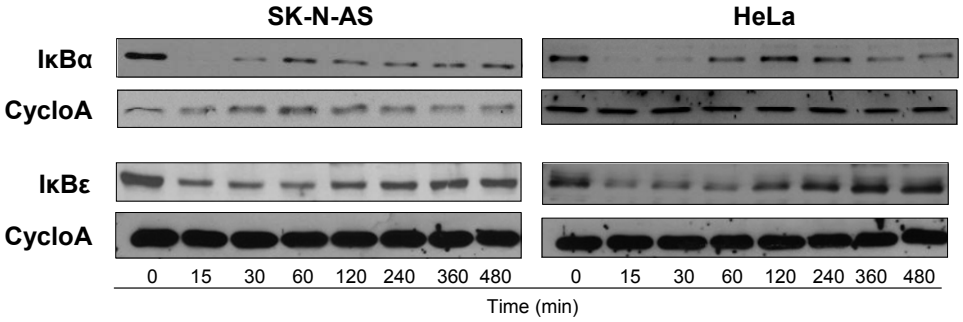

Fig. S11: Western blot analysis of IκBα and IκBε protein levels in SK-N-AS and HeLa cells. *SK-N-AS and Hela cells treated with continuous 10 ng/ml TNFα, lysed at the indicated times and analysed for IκBα, IκBε and Cyclophilin A (cyclo A) protein levels.*

The origin of the differential transcriptional control of IκBα and IκBε genes was investigated. RelA was transiently bound to both IκBα and IκBε promoters upon stimulation (Fig. 3C and Fig. S12A). RNA polymerase II was bound to the respective promoters (Fig. 3D) at different times. In contrast, RNA polymerase II was not bound to a control DNA region (Fig. S12C).

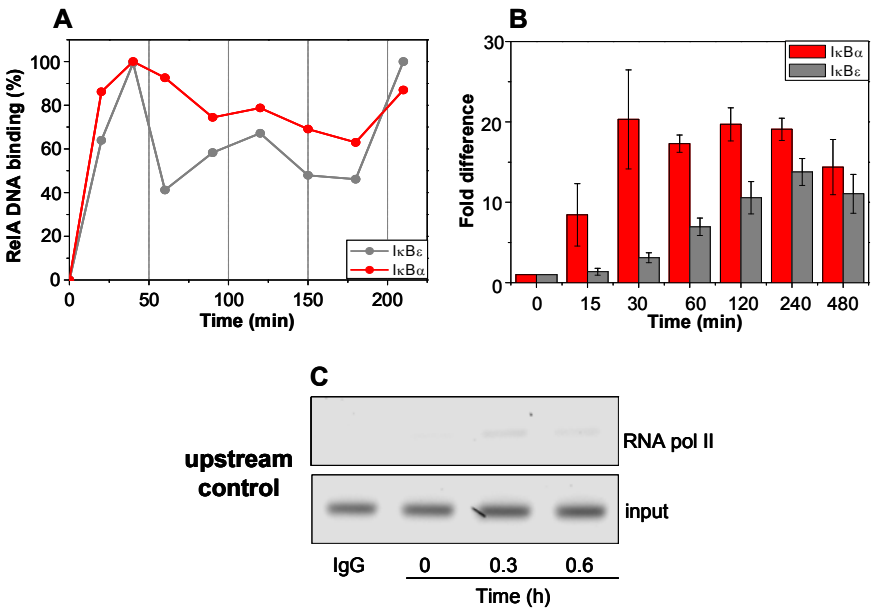

Fig. S12: DNA binding and transcription analysis of IκBα and IκBε. *(A) ChIP analysis of RelA DNA binding levels at the IκBα and IκBε promoters in SK-N-AS cells after continuous 10 ng/ml TNFα stimulation. Densitometric analysis of the data in Fig. 3C with binding levels normalised to the highest intensity. (B) Quantitative RT-PCR analysis of IκBα and IκBε gene expression in SK-N-AS cells after continuous 10 ng/ml TNFα stimulation. Shown are averages (±SD based on 2 replicates). (C) ChIP analysis of RNA polymerase II DNA binding levels at a region on the IκBα promoter ~1000 bp upstream of the ATG in SK-N-AS cells after continuous 10 ng/ml TNFα treatment.*

Efficient knock-down of the IκBε protein was achieved during imaging experiments using a specific siRNA (Fig. S13) as confirmed by Western blotting of the same cells (Fig. S13 right panel).

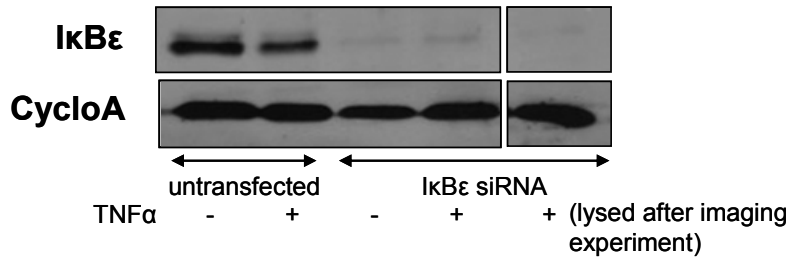

Fig. S13: IκBε protein levels in untransfected and IκBε siRNA transfected SK-N-AS cells in the presence or absence of TNFα. *IκBε siRNA untransfected or transfected cells were treated with TNFα for 4.5-hours (48-hours post-plating) and the protein level quantified. Cells transfected with RelA-dsRedxp and IκBε siRNA (48-hours post-plating), were stimulated for ~16-hours with TNFα whilst being imaged by confocal microscopy and subsequently analysed for IκBε and cyclophilin A by western blotting,*

Single cells continuously stimulated with 10 ng/ml TNFα exhibited persistent N:C RelA oscillation for both control, (Fig. 3G and Fig. S14D) as well as IκBε knock-down (Fig. 3H) conditions. Significant heterogeneity between individual cells resulted in damped population level response (Fig. S14A-C). We noted that model simulations for IκBε knock-down over a range of NF-κB levels (4-fold) showed a decrease of cell-to-cell synchronization associated with an increase in NF-κB expression (Fig. S15E-H). By contrast, in the wild-type we found slightly increased synchronization when NF-κB expression was increased (Fig. S15A-D), with the optimal IκBε-mediated damping at the population level occurring at a level of 60,000 NF-κB molecules (Fig. 3 and Fig. S16C-F).

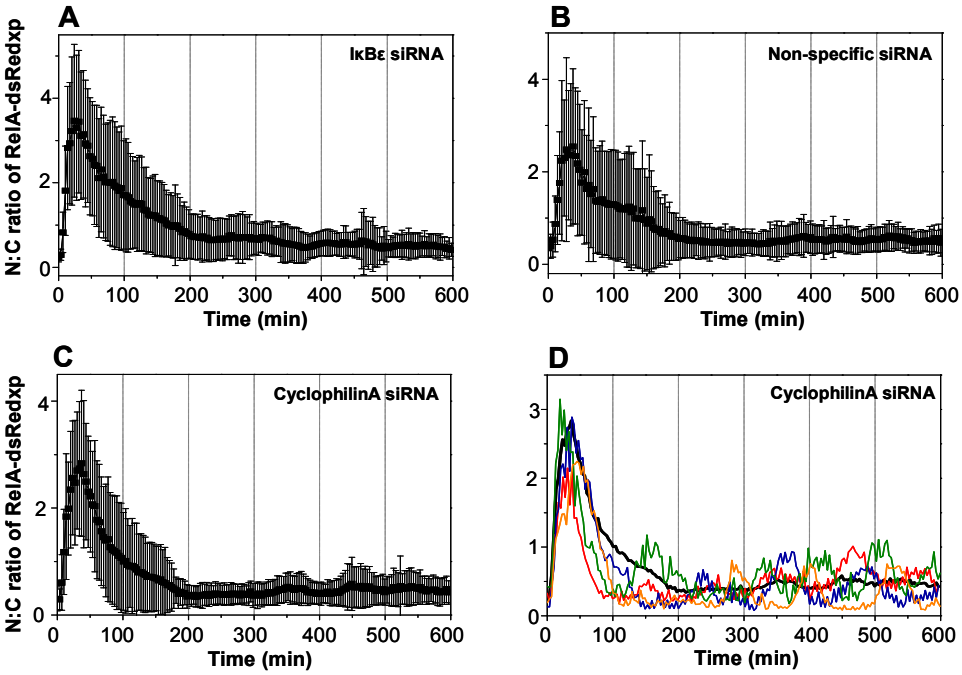

Fig. S14: Analysis of RelA-dsRedxp dynamics in siRNA transfected cells. *(A, B & C) Time course of cell population average (±SD) of N:C localisation of RelA-dsRedxp in SK-N-AS cells co-expressing either (A) IκBε (n=61), (B) non-specific (n=57) and (C) cyclophilin A (n=36) siRNA after continuous 10 ng/ml TNFα stimulation. (D) Time course of N:C localisation of RelA-dsRedxp in SK-N-AS cells transiently transfected with RelA-dsRedxp and Cyclophilin A siRNA after continuous 10ng/ml TNFα stimulation. Four representative single cells are displayed by a different coloured line and the average population response is shown by a black line.*

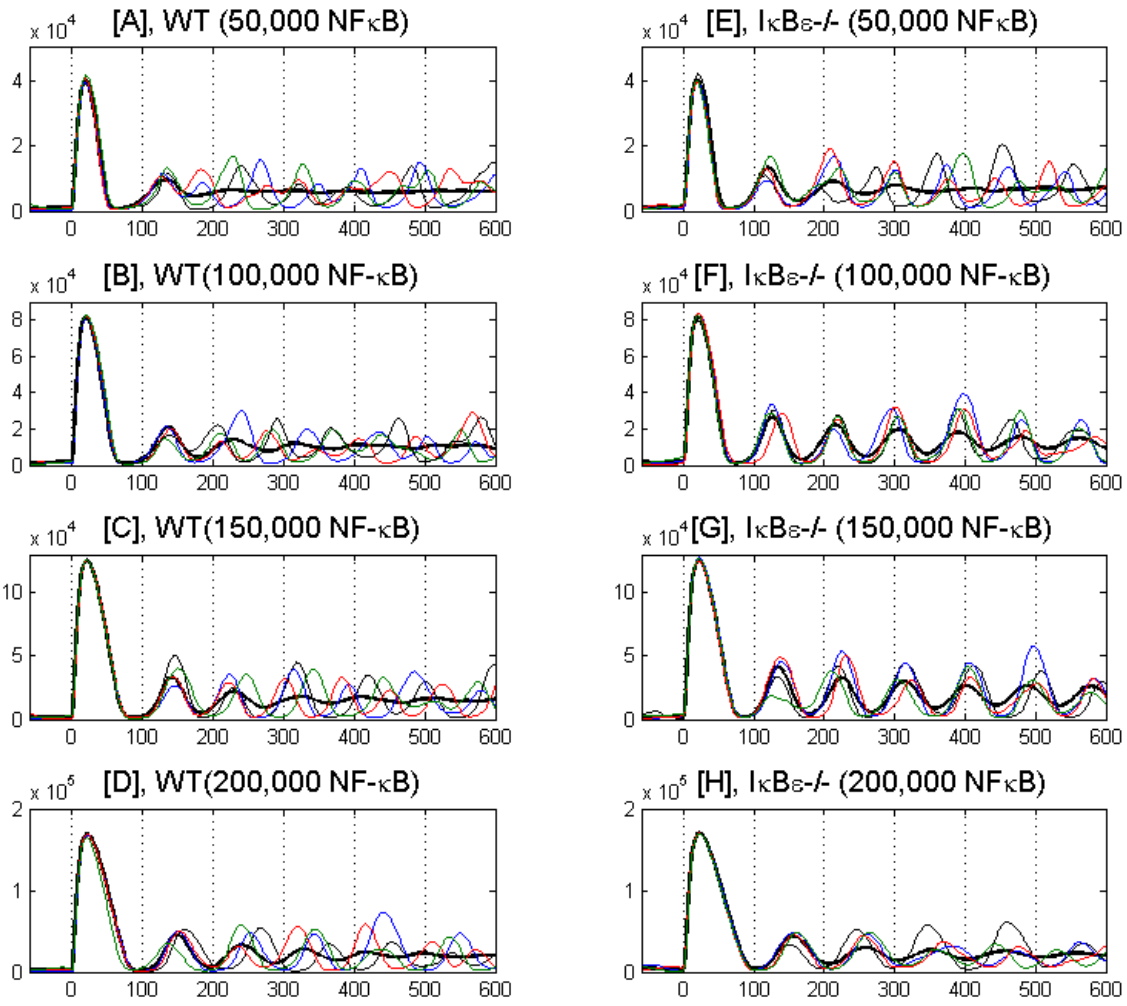

Fig. S15: Effect of different NF-κB levels on oscillations in nuclear NF-κB level following continuous TNFα stimulation. *Single cell vs. population dynamics in (A-D) wild-type (WT) and (E-H) IκBε knock-out (IκBε-/-) simulated cells. Each subplot shows four representative single cell trajectories augmented with the average trajectory calculated based on 100 simulated cells. TNFα treatment was introduced at time t=0 minutes and sustained until the end of the simulated experiment. (A, E) 50,000, (B, F) 100,000, 150,000 (C, G) and (D, H) 200,000 NF-κB molecules per cell were tested.*

TNFα-stimulated single cells oscillated with a period of ~100-minutes (Fig. S16A), but more importantly we found that their oscillation amplitude was not affected by IκBε knock-down (Fig. S16B). The amplitude and timing of simulated single cells oscillations (Fig. 3E & F) were in qualitative agreement with the experimental data, despite markedly reduced variability of Peak1 amplitude and Time0:Peak1 timing in the model (Fig. S16C & D). Further analysis of the simulated single cell peak-to peak timing might explain the different levels of synchronisation in wild-type cells compared to those with the IκBε knocked-down. We found that variability in the RelA period, but not nuclear amplitude was significantly reduced in the IκBε knock-down cells (Fig. S16E & F). As a result, single IκBε knock-down cells were more synchronized than the wild-type. This

synchronization is also exhibited by narrower peak-to-peak timing distributions (Fig. S17 vs. Fig. S18, corresponding distributions measured experimentally are depicted in Fig. S19,Fig. S20 andFigure S21).

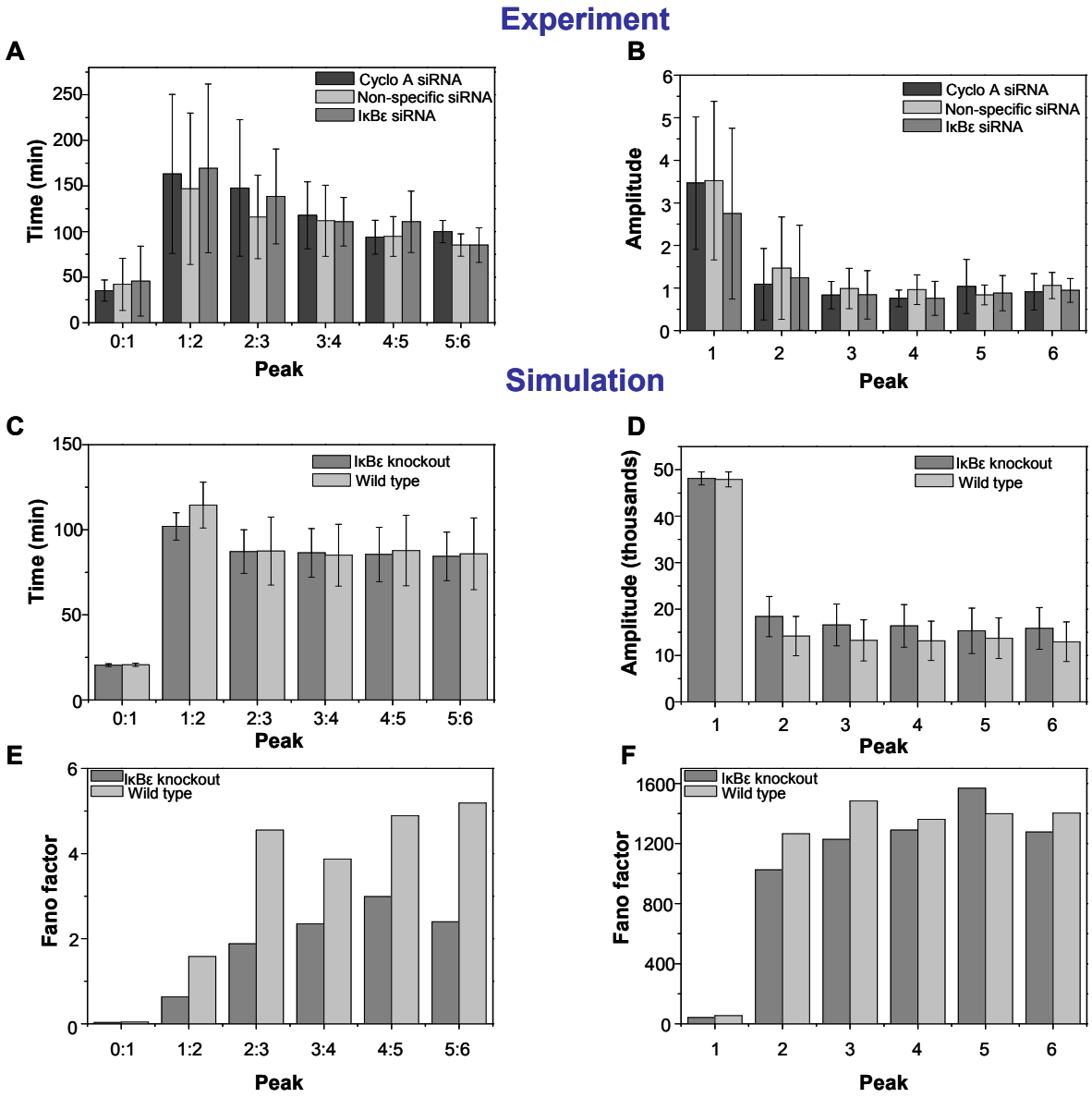

Fig. S16: Analysis of single cell NF-κB oscillations following continuous TNFα stimulation. *(A & B) Experimentally determined average (A) timing between successive peaks and (B) amplitude (N:C ratio) (±SD) of RelA-dsRedxp translocations following cyclophilin A, non-specific and IκBε siRNA knock-down conditions in SK-N-AS cells. (C & D) Simulations (for total of 60,000 NF-κB molecules). (C) Timing between successive peaks and (D) amplitude of NF-κB in wild type and IκBε knock-out conditions based on 100 single cells. (E) Fano factor calculated for timing between successive peaks in (C). (F) Fano factor calculated for peak nuclear amplitudes in (D).*

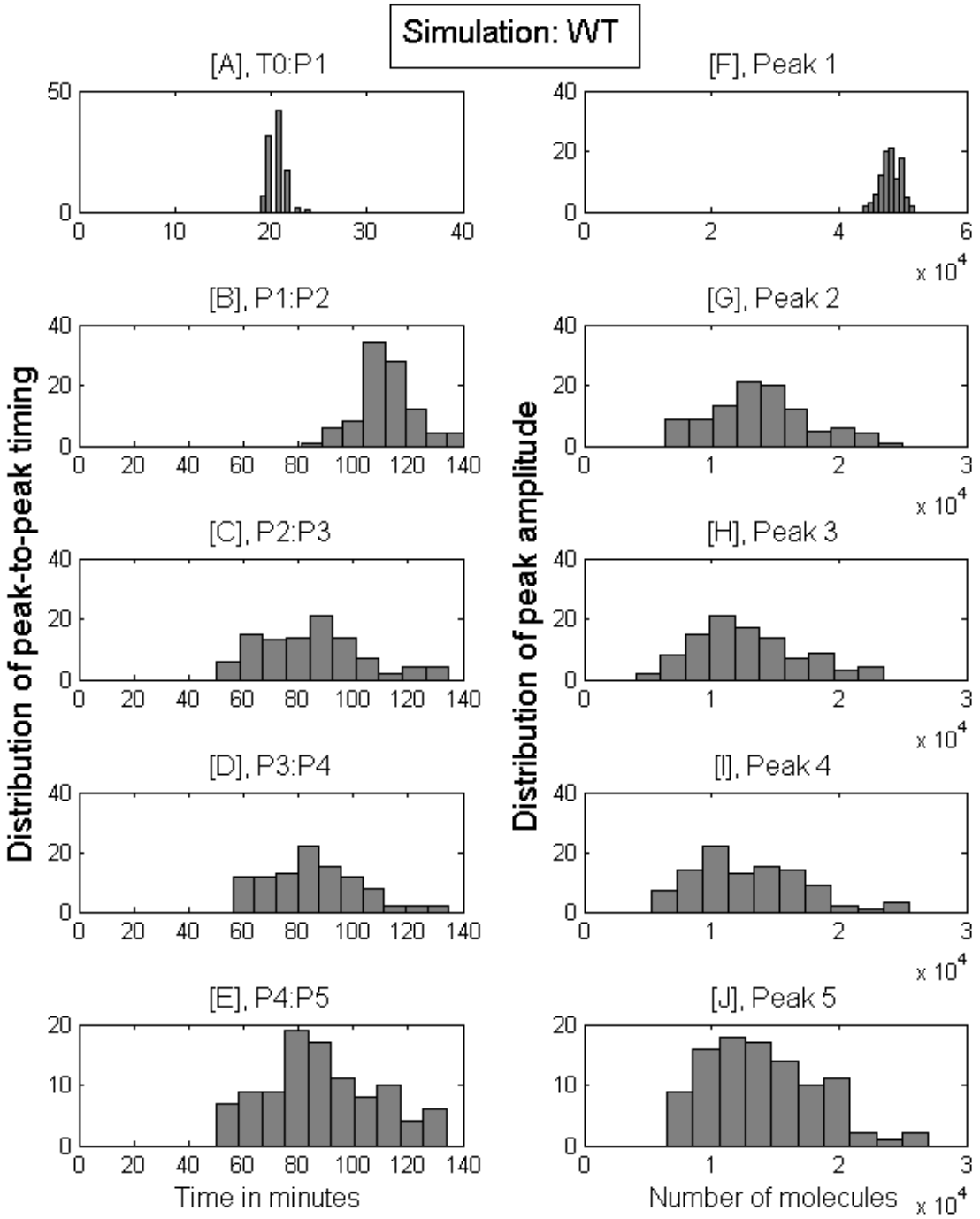

Fig. S17: Distribution of peak-to-peak timing (A-E) and peak amplitude (F-J) in IκBε wild-type for simulated data in Fig. 3E.

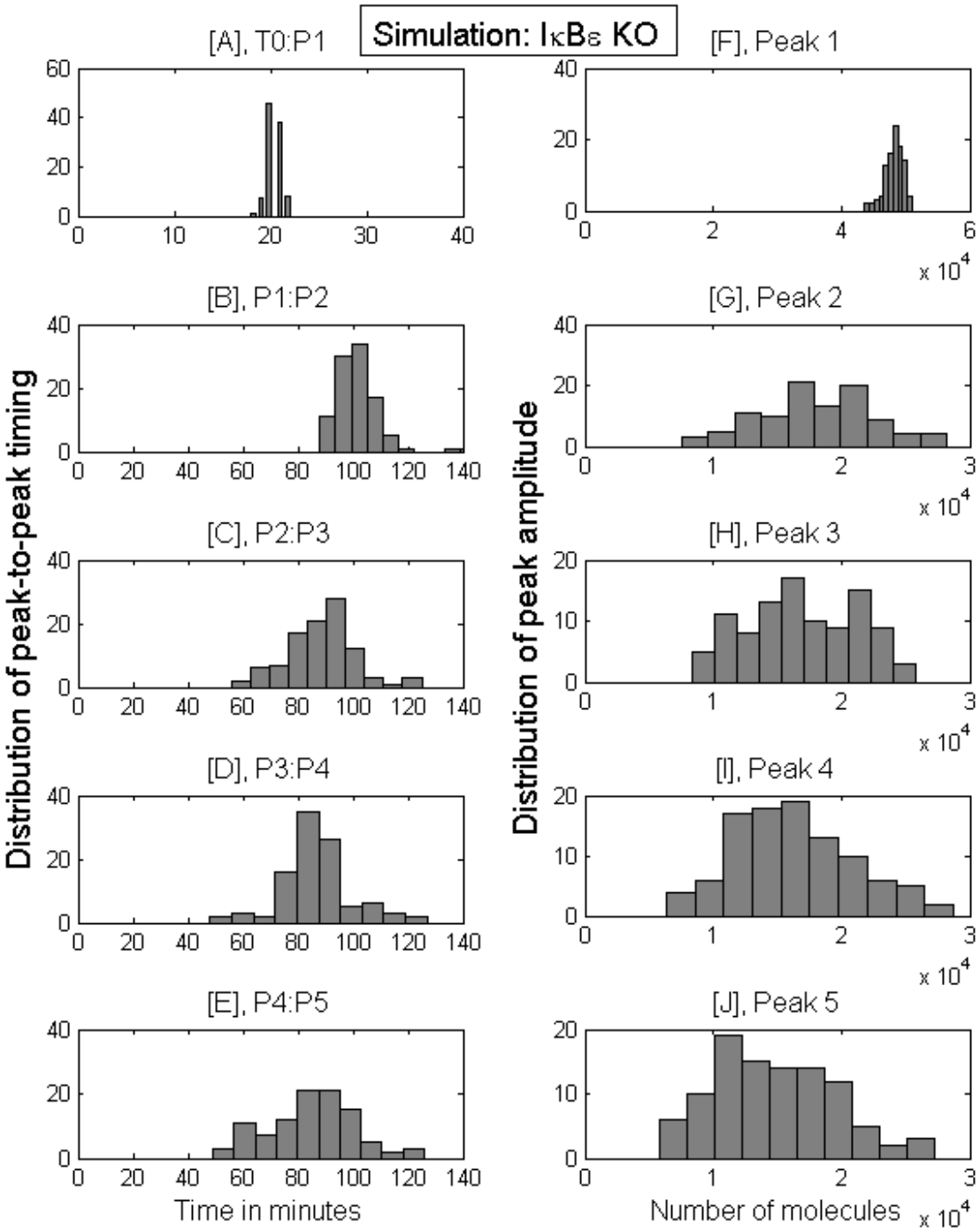

Fig. S18: Distribution of peak-to-peak timing (A-E) and peak amplitude (F-J) in IκBε knock-down for simulated data in Fig. 3F.

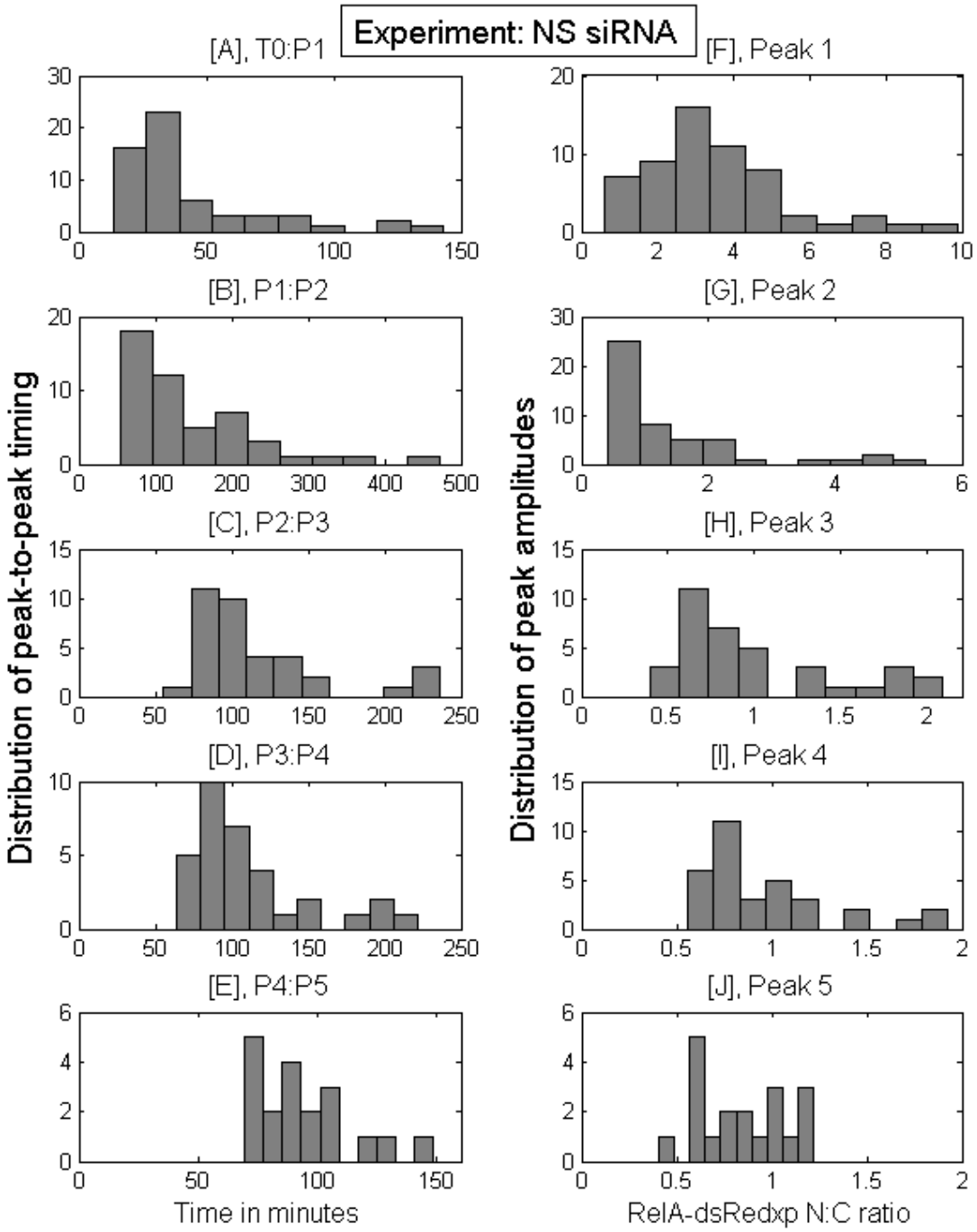

Fig. S19: Distribution of peak-to-peak timing (A-E) and peak amplitude (F-J) calculated for data in Fig. 3G.

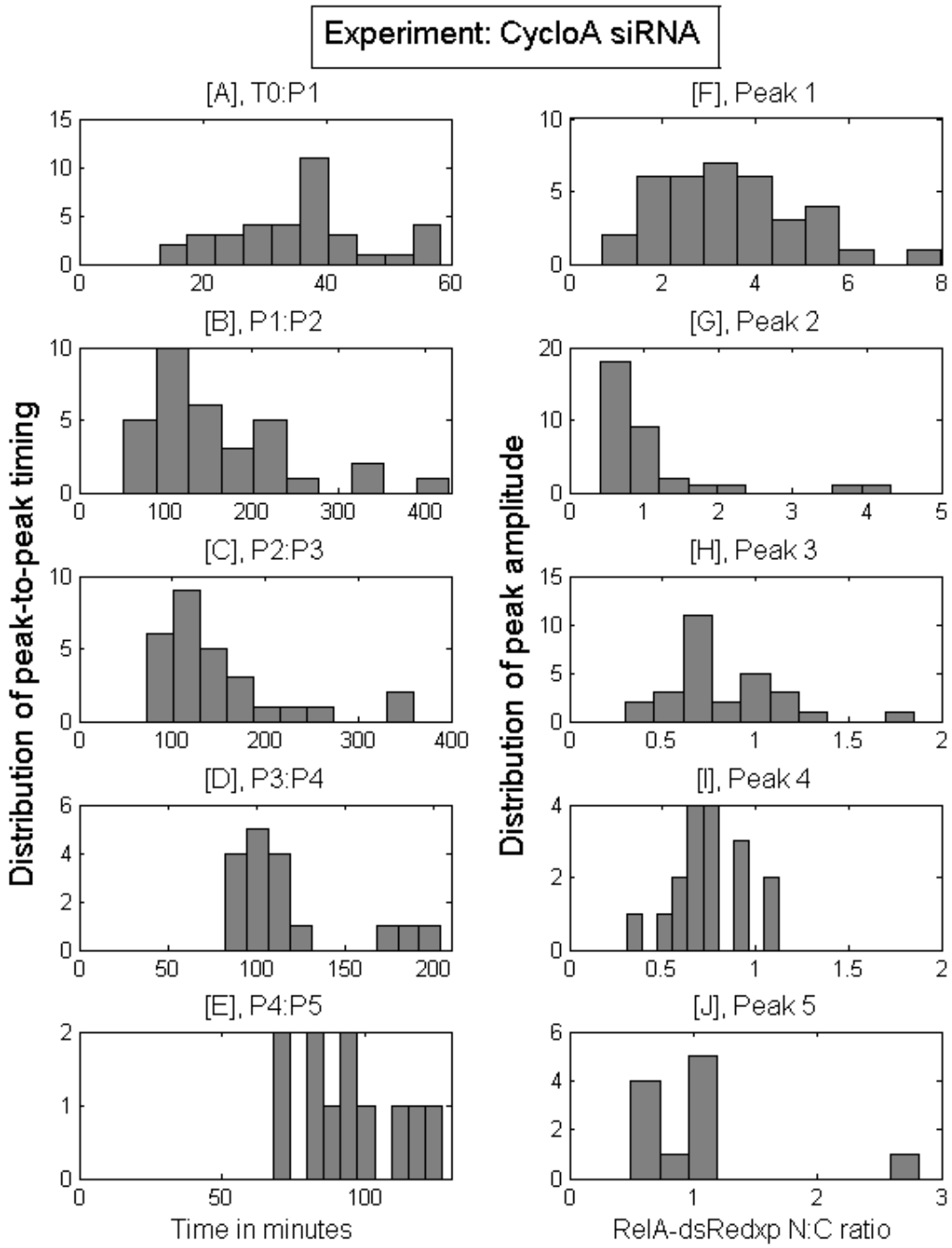

Fig. S20: Distribution of peak-to-peak timing (A-E) and peak amplitude (F-J) calculated for data in Fig. S14D.

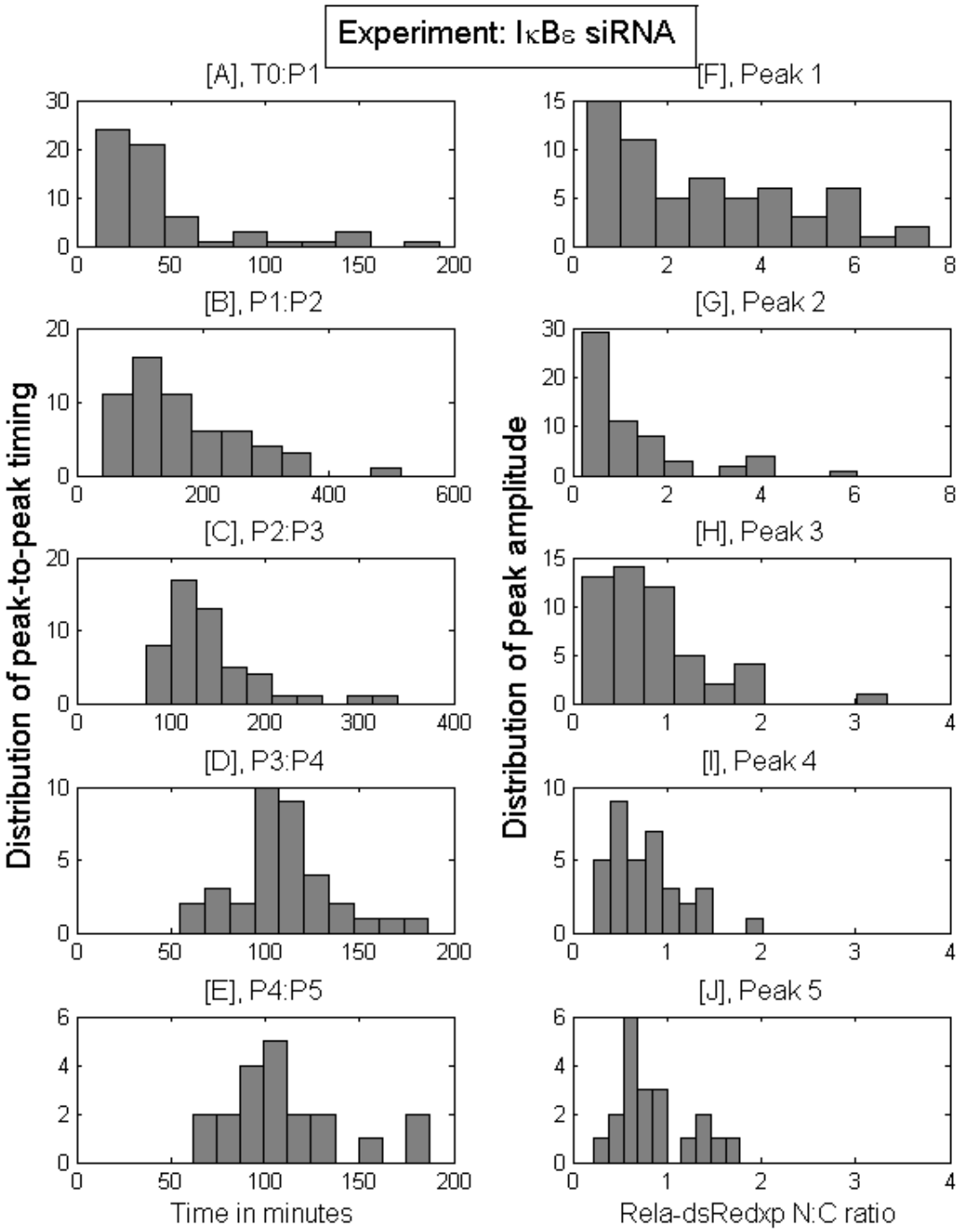

Figure S21: Distribution of peak-to-peak timing (A-E) and peak amplitude (F-J) calculated for data in Fig. 3H.

RelA expression was analysed following transfection in unstimulated cells (Fig. S22A top left panel) to investigate the effect on the relative IκBα and IκBε expression levels. The total RelA level increased 1.8-fold after stable transfection and about 4-fold after transient transfection both in unstimulated and 5-hours after continuous TNFα stimulation (Fig. S22A-D). Increased expression of RelA in transfected cells resulted in increased levels of IκBα and IκBε protein in unstimulated and TNFα stimulated cells (Fig. S22A & B bottom panels). We found that IκBα and IκBε were up regulated to similar degree (2.8 and 2.0 fold, respectively compared with untransfected control, Fig. S22E & F). These experiments confirmed that neither stable nor transient RelA-dsRedxp expression changed the normal ratio of IκBα and IκBε.

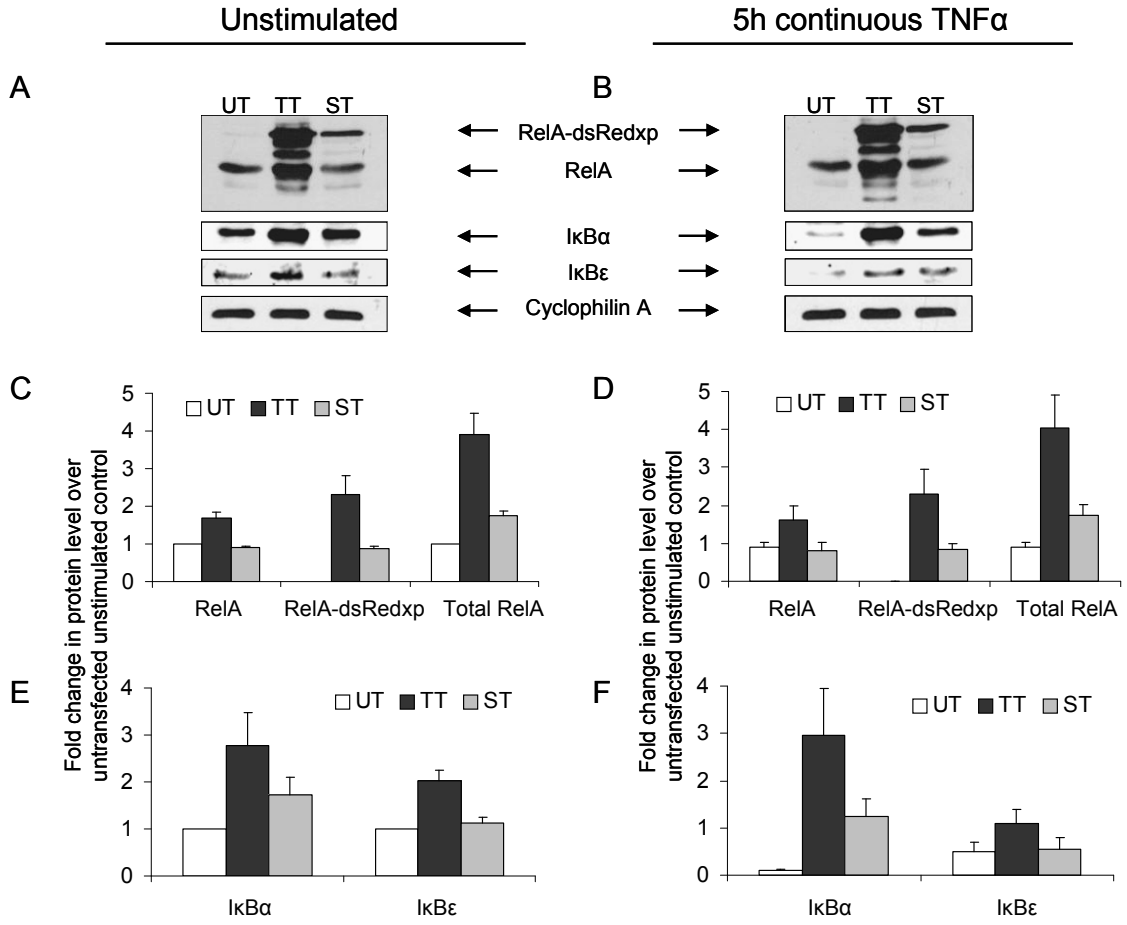

Fig. S22: Western blot analysis of IκBα and IκBε protein levels in RelA-dsRedxp transfected SK-N-AS cells. *(A & B) protein levels in untransfected (UT), transiently transfected with RelA-dsRedxp (TT) and stably transfected with RelA-dsRedxp (ST) SK-N-AS cells under (A) unstimulated conditions or after (B) 5-h continuous 10 ng/ml TNFα stimulation. Quantification of data in C & E under unstimulated conditions and (D & F) after 5-h continuous 10 ng/ml TNFα stimulation (averages (±SD) based on 2 replicates).*

Section D: Function of NF-κB oscillation frequency.

We used ChIP assays to show that both 200- (Fig. 4B) and 100-minute (Fig. S23A) repeat pulsing induced waves of RelA binding at the IκBα promoter at the input frequency. We observed that high oscillation frequency was required for expression of late (RANTES and MCP-1), but not early genes (IκBα and IκBε) using quantitative RT-PCR (Fig. 4C-H). This was initially observed with semi-quantitative RT-PCR (Fig. S23B), which showed markedly increased expression of RANTES at 100- comparing to 200-minute input frequency.

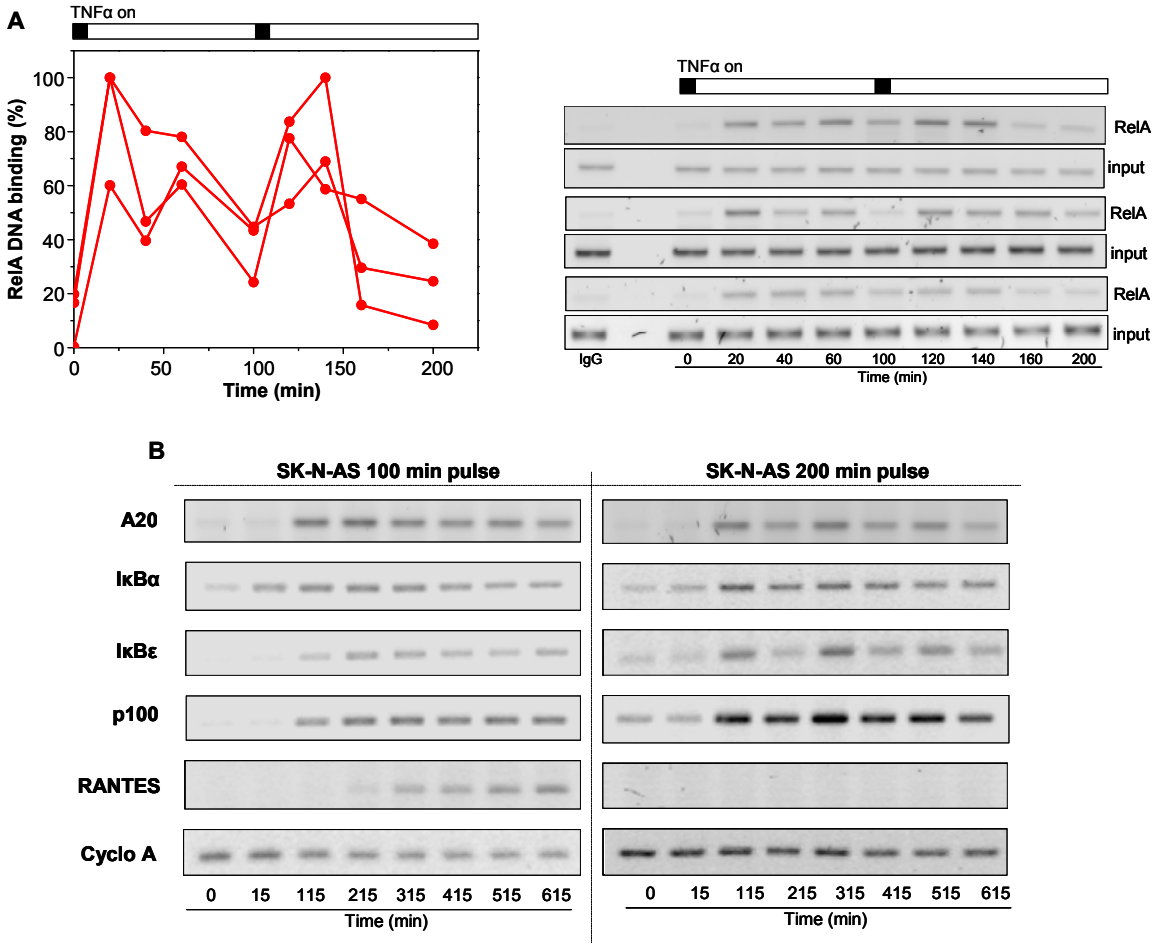

Fig. S23: Analysis of RelA DNA binding and resulting gene expression. *(A) ChIP analysis of RelA DNA binding levels at the IκBα promoter in SK-N-AS cells after a repeated 5-minute TNFα pulse at 100-minute intervals. Graphs show densitometric analysis of the replicate gels with binding levels normalised to the highest intensity. (B) Semi-quantitative RT-PCR for early (A20, IκBα), middle (IκBε, p100) and late (RANTES) gene mRNA expression after 5-minute TNFα pulsing at 100- and 200-minute frequencies.*

3. Mathematical modeling

Section A: Deterministic 2-feedback NF-κB model: Existing models were tested for their ability to predict observed NF-κB responses to varying TNFα stimulation profiles within the same cell system (continuous (*1*), single pulses of varying duration (Fig. S7), and 5-minute repeat pulses with varying frequency (Fig. 2 and Fig. S3)).
Models tested include Hoffmann *et al.,* (2002), and its simplified version (IκBα isoform only with assumptions from (*10*)). These were able to predict observed NF-κB amplitude sensitivity to TNFα pulse duration (Fig. S7). However, simulation of repeat pulse experiments in this model (IKKa wash rate following each pulse, *k02*=0.003 s^{-1}) were extremely sensitive to excess *de novo* IκBα protein levels, which prevented NF-κB activation to a second equivalent TNFα/IKK pulse for all tested intervals (60-, 100- and 200-minute).
These models as well as other derivatives of the Hoffmann *et al.*, (2002) (*9, 11-13*) were lacking an explicit representation of the IKK structure. An explicit representation of the IKK structure was proposed by Lipniacki *et al.*, (2004 and 2006), based on measurements for IKK activity with continual TNFα (*14*). The corresponding model was unable to simulate repeated 5-minute TNFα pulsing experiments, and also showed no NF-κB peak amplitude variation to TNFα pulse duration (in contrast to imaging experiments (Fig. S7)) (IKK was predicted to be invariant for these conditions). To formulate a model which could fit all TNFα stimulation conditions, the Base and IKK modules were initially considered separately (Fig. 2E).

Base Module (see Fig. 2E)**:**
The scope of the base module involved variables describing the nuclear and cytoplasmic free and complexed forms of NF-κB, IκBα and IκBα mRNA (tIκBα) (7 variables in total). Each model variable was represented by an ordinary differential equation (see Table S7). Parameter values from existing models were modified if relevant experimental measurements from SK-N-AS cells were available, any parameters supported by experimental evidence were retained, and remaining parameters were fitted (as referenced). The structure of the NF-κB-IκBα (Base) module was similar to many existing models in the literature (*15*) (summarised in Table S1).
Spatial considerations Molecular species were spatially segregated between nuclear and cytoplasmic cellular compartments. Different compartmental volumes were accounted for when calculating molecular concentrations and transport rates were appropriately scaled by the ratio of cytoplasmic to nuclear volumes (*kv*). This ratio alters nuclear NF-κB concentration, which has a direct impact on IκBα synthesis (an extremely sensitive parameter (*1, 10*)). *kv* was estimated for SK-N-AS cells using 3D confocal microscopy of trypsinised cells expressing 2 different colored fluorescent fusion proteins restricted to each respective compartment. This gave an average of 3.3 (±1.2 SD), also the total cell volume (*tv*) was measured at 2671 μm^3 (± 851 SD), and rounded to 2700 μm^3 (Table S1), these parameters were fixed.

Reaction	Symbol	Value	References
Spatial parameters			
Total cell volume	*tv*	2700 μm^3	Measured
C:N ratio	*kv*	3.3	Measured
Conversion to nuclear volume	*nv*	×(kv+1)	-
Conversion to cytoplasmic volume	*cv*	×(1/kv+1)	-
Initial concentration			
Total NF-κB	NF	0.08 μM	Initialized as cytoplasmic IκBα·NF-κB
Complex formation & dissociation			
IκBα + NF-κB → IκBα·NF-κB nIκBα + nNF-κB → nIκBα·NF-κB	*ka1a* *ka1an*	0.5 $\mu M^{-1}s^{-1}$	(*16*)
IκBα·NF-κB → IκBα + NF-κB nIκBα·nNF-κB → nIκBα + nNF-κB	*kd1a*	0.0005 s^{-1}	(*16*)
IκBα protein synthesis & degradation			
nNF-κB → nNF-κB + tIκBα *Order of hill function, h=2* *Half-max constant, k=0.065^h(fitted)*	*c1a*	1.4×10^{-7} $\mu M^{-1}s^{-1}$	Fitted (constrained): 1.07×10^{-7} – 8.2×10^{-7} $\mu M^{-1}s^{-1}$ (*17*), (*11*)
tIκBα→ tIκBα + IκBα	*c2a*	0.5 s^{-1}	(*8*)
tIκBα→ Sink	*c3a*	0.0003 s^{-1}	Fitted (constrained): 0.00077-0.00029 s^{-1} (*18*)
IκBα→ Sink	*c4a*	0.0005 s^{-1}	Fitted (constrained): 0.000105 – 0.002 s^{-1} (*12, 19, 20*)
NF-κB·IκBα→ NF-κB	*c5a*	0.000022 s^{-1}	(*19, 20*)
nNF-κB·nIκBα→ nNF-κB	-	0 s^{-1}	Assumed (*12, 19*)
Transport			
NF-κB → nNF-κB	*ki1*	0.0026 s^{-1}	Measured fitting range: *Average 0.0026 ± 0.0018 s^{-1}*
nNF-κB → NF-κB	*ke1*	0.00052 s^{-1}	*ki1*/50 (*21*)
nIκBα·nNF-κB → IκBα·NF-κB	*ke2a*	0.01 s^{-1}	Fitted
IκBα → nIκBα	*ki3a*	0.00067 s^{-1}	Measured fitting range: Average *0.00043 ± 0.00024 s^{-1}*
nIκBα → IκBα	*ke3a*	0.000335 s^{-1}	*ki3a*/2 (*21*)

Table S1: Base module reactions and associated parameters.

Initial NF-κB levels A value of 100,000 molecules per SK-N-AS cell was assumed, which gave a total cell concentration of 0.06 μM (equivalent to respective cytoplasmic and nuclear concentrations of 0.08 μM and 0.26 μM).

Protein synthesis In the deterministic description, transcription from NF-κB-inducible promoters was assumed to be dependent on the level of nuclear NF-κB. This process was modeled as a second order Hill function (*9*). By assigning the transcription rate as the maximum possible rate of mRNA production from two gene copies (*c1a*), the Hill function determines the fraction of maximal production occurring at any time, based on nuclear NF-κB levels relative to the half-maximal constant (*k*): $c1a \times (nNF\text{-}\kappa B^2 / (NF\text{-}\kappa B^2 + k^2))$. This accounted for transcription saturation with high NF-κB concentrations, and could therefore correctly predict the insensitivity of the NF-κB oscillation period to increasing NF-κB expression levels (*10*). A second order Hill function was assumed for both IκBα and A20 gene activity as there are 2 required NF-κB binding sites on each promoter (*22, 23*). This second order dependence was not essential for model kinetics (a

similar fit is possible with adjustment of *h=1* and *k=0.043*, for the Base-Proposed IKK structure). The maximal rate of transcription initiation frequency was considered to be within the range of 0.067 s^{-1} (4 mRNA/min (*17*)) to 0.55 s^{-1} (33 mRNA/min (*11*)) per gene. Therefore, we considered the range for the maximal cytoplasmic mRNA production rate from two genes as 1.07×10^{-7} $\mu M^{-1}s^{-1}$ to 8.2×10^{-7} $\mu M^{-1}s^{-1}$ (scaled by ~$1.2x10^{6}$ molecules representing 1 μM cytoplasmic concentration). Constitutive transcription was fixed at zero for simplicity.

Constitutive IκBα protein turnover, free and complexed This model discriminated only between free and NF-κB(RelA)-complexed IκBα. The half-life of free IκBα was measured to be 110-minutes (*20*). Most likely this measurement constrained a lower bound for fitting, since the half-life of IκBα was reported to be ~10-minutes in $nfkb1^{-/-}$ $rela^{-/-}crel^{-/-}$ cells (*12, 19*). We assumed that constitutive IκBα degradation was IKK-independent and that it occurred in both the cytoplasm and nucleus with a half-life of 23-minutes (fitted in parallel with tIκBα stability). NF-κB-complexed IκBα turnover was assumed to be 8- to 9-h (*19, 20*). This rate has been proposed to be dependent on basal IKK activity (*12*), it was therefore assumed this was a cytoplasmic event.

IκBα mRNA stability Existing experimental measurement of IκBα mRNA stability was used to constrain fitting between 0.00077-0.00029 s^{-1} for a half-life of 15-40 minutes (*18*). The final fit of this parameter (half-life of 38 minutes) was performed upon integration of the IKK and Base modules based on measurements following a 5-minute TNFα pulse (Fig. S24).

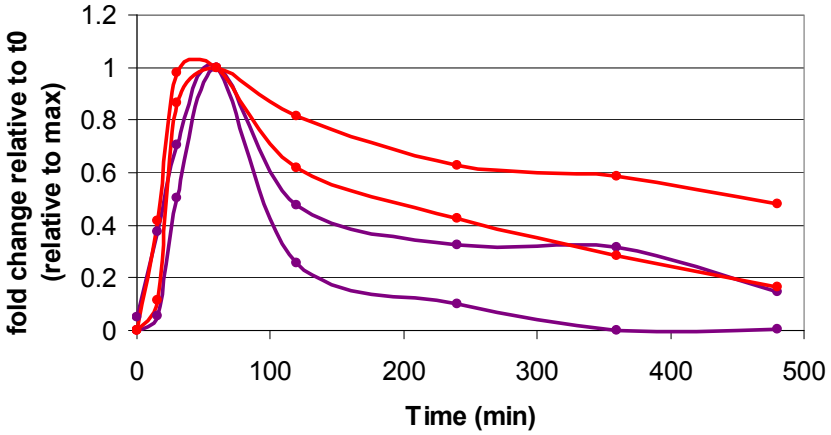

Fig. S24: RT-PCR analysis of IκBα and A20 mRNA levels in SK-N-AS cells following a 5-minute TNFα pulse. *Red lines IκBα and purple lines A20 PCR products analysed by densitometry of agarose gel electrophoresis. The proportion fold change was normalized to cyclophilin A PCR products at time 0.*

NF-κB and IκBα transport NF-κB import was estimated in RelA-dsRedxp expressing cells treated with Leptomycin B and TNFα (0.0026 ± 0.0018 s^{-1}). Similarly, IκBα import in cells expressing IκBα-EGFP in the absence of TNFα was estimated (0.00043 ± 0.00024 s^{-1}) (Fig. S25).

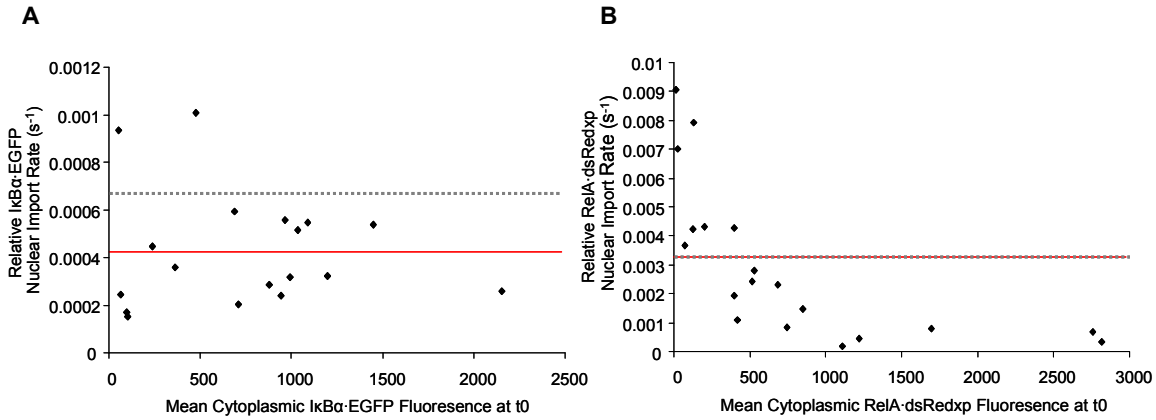

Fig. S25: Analysis of IκBα-EGFP and RelA-dsRedxp nuclear import rate in SK-N-AS cells. *SK-N-AS cells co-transfected with (A) IκBα-EGFP and dsRedxp, or (B) RelA-dsRedxp and pEGFP-N1. 24-h post-transfection, cells were treated with 10ng/ml LMB (A), or 10ng/ml LMB and TNFα (B). Relative nuclear import rate was calculated for each cell as the rate of increase in nuclear fluorescence during the approximate linear phase normalised to the initial cytoplasmic fluorescence (21). The fitted import rates (grey) used in all computational models were 0.00067s^{-1} (A) and 0.0026s^{-1} (B), taken from the measured ranges defined by the average (red) ±1SD, of 0.00043±0.00024s^{-1} (A) and 0.0026±0.0018s^{-1} (B). (B) Due to the dependence of RelA-dsRedxp level on relative import rate in TNFα stimulated cells, the top/bottom 10% of measurements were removed from the final statistics.*

Interaction with the IKK Module:

The Base module interaction with the IKK module occured via IKK-induced phosphorylation and degradation of IκBα and IκBα·NF-κB (Table S2). This reaction structure and parameter values were fixed for both the existing (Fig. 2F) and proposed IKK modules (Fig. 2G).

IκBα phosphorylation Measurements by Heilker *et al.* (1999) and Zandi *et al.* 1998 (*24, 25*) were in agreement with imaging experiments (*1, 26*). More recently, it was proposed that the NF-κB-bound IκBα phosphorylation may be as efficient as that of free IκBα (*19*). However, rescaling *kc1a* to equal *kc2a* led to reductions in both oscillation period and stable peak amplitudes that did not fit observations. To simulate repeat pulse experiments the initial IKK activity was required to be high, therefore these parameters were increased two fold to allow sufficient degradation of IκBα (14.0 % ±12.3 (SD) of initial levels by 5-minute post TNFα stimulation, Fig. S5 and Fig. S6).

Reaction	Symbol	Value	References
Base Module IKK Interacting Parameters			
IKKa + IκBα → pIκBα	*kc1a*	0.074 s^{-1}	Assumed (0.037×2) (*24*)
IKKa + IκBα·NF-κB → pIκBα·NF-κB	*kc2a*	0.185 s^{-1}	Assumed (0.037×5×2) (*24, 25*)
pIκBα → Sink	*kt1a*	0.1 s^{-1}	Fitted
pIκBα·NF-κB → Sink	*kt2a*	0.1 s^{-1}	Fitted

Table S2. Reactions and associated parameters integrating Base and IKK modules.

IKK Module:
The IKK modules investigated (Fig. 2F & G) included three states of IKK activity represented as IKKn, IKKa, IKKi, (*8*) as well as A20 protein and transcript, tA20; all were assumed to be exclusively cytoplasmic.

1. IKKn: A neutral IKK, capable of being activated by upstream signals.
2. IKKa: An active IKK, which can activate NF-κB by phosphorylating IκBα (produced from IKKn at a rate *ka* in the presence of TNFα, and inactivated at a rate *ki*).
3. IKKi: An inactive IKK, unable to be activated or phosphorylate IκBα (produced from IKKa at a rate *ki*).

New constraints on IKK structure required that IKK activation was reset after a 200-, but not 100- and 60-minute interval following a single 5-minute TNFα pulse (Fig. 2D).

Existing IKK structure A20 inhibition (*kiA20*) increased the rate of IKKa inactivation into IKKi, and was dependent on the presence of TNFα (Table S3).

Reaction	Symbol	Value	References
TNFα stimulation			
TNFα	TR	1/0	on/off (*8*)
IKK parameters			
Source → IKKn	***kp***	**0.00004 s^{-1}**	**Assumed, kp/kd = NF**
IKKn/IKKa/IKKi → Sink	***kd***	**0.0005 s^{-1}**	**Fitted, based on 200 min reset following a 5-min TNFα pulse**
IKKn → IKKa	*ka*	0.003 s^{-1}	Fitted
IKKa → IKKi	*ki*	0.002 s^{-1}	Fitted
A20 + IKKa → A20 + IKKi	***kiA20***	**0.215 s^{-1}**	**Fitted, dependent on receptor state *kiA20×TR***
A20 protein synthesis & degradation			
nNF-κB → nNF-κB + tIκBα *Order of hill function, h=2* *Half-max constant, k=0.065^h(fitted)*	*c1*	1.4×10^{-7} $\mu M^{-1}s^{-1}$	Assumed to be the same as IκBα
tA20→ tA20 + A20	*c2*	0.5 s^{-1}	(*8*)
tA20→ Sink	*c3*	0.00048 s^{-1}	Fitted (constrained): > tIκBα turnover (Fig. S24).
A20 → Sink	*c4*	**0.00143 s^{-1}**	Best fit

Table S3: Existing IKK Module reactions and parameters. *The reactions and parameters marked in bold are different between the IKK modules.*

Modification of IKK parameters The ability for this structure to faithfully reproduce a response from a 5-minute TNFα pulse required modification of IKK parameters. Following removal of TNFα the only parameter controlling the IKK reset rate was *kd*, a minimum value which allowed complete restoration of IKKn was 0.0005 s^{-1}. The total IKK level in this model was conserved through *kp*/*kd*, and we assume that it was equal to the total NF-κB concentration. Modifications to *ka* and *ki*, were made to simulate IKK activity (IKKa) based on experimental observations, where available. Maximum IKK

activity (with/without A20) was assumed to occur between 5- to 10-minute post stimulation with continual TNFα (10 ng/ml), and reached a tail level by ~30-minute following the initial activation peak (*11, 14*). IKKa peak amplitude and time was sensitive to *ka*, whereas amplitude, duration and level of the activation 'tail' (crucial for controlling N:C NF-κB oscillation dynamics) depended on *ki*. To account for A20 feedback, *ka* and *ki* were fitted following integration of the Base and IKK modules.

A20 mRNA A20 transcript decayed at a faster rate than IκBα (fitted half-lives of 24- and 38-minutes respectively in the model) following a 5-minute TNFα pulse (Fig. S24). A20 protein parameters were fitted following integration of the Base and IKK modules.

Limitations of the existing model Simulation of a single/repeated 5-minute pulse (Fig. S6) required sufficient IκBα degradation by IKKa, in contrast to continuous TNFα stimulation which required a low tail of later IKK activity (or relatively stronger negative feedback). These features imposed incompatible constraints on the existing structure (Fig. S8). With sufficient initial IKK activity to degrade IκBα, A20 inhibition was essential to decrease tail IKK activity in continuous TNFα simulations. However, repeated pulse experiments were extremely sensitive to this high level of A20 inhibition. Even an A20 protein with very short half-life but capable of strong inhibition was inadequate since it blocked any NF-κB responses from a repeated 5min TNFα pulse at 60-minutes (Fig. S8).

Proposed IKK module:

Inhibition of *kp* by A20 (in the presence of TNFα), instead of inactivating IKKa, in the existing IKK module was able to simulate IKKa profiles to satisfy all conditions. However, A20 diminished total IKK levels over time (contradictory to observations by (*14*)). A model proposed by Hacker and Karin, 2006 provided a view of cycling in IKK activity state based on regulation by autophosphorylation (*27*). Thus it was assumed that IKKn was produced from the pool of IKKi with a rate *kp*; and that no IKK degradation (*kd*=0) occurred. The target for A20 was IKKi and it was also assumed that A20 inhibited reactivation of IKK by reducing the rate of conversion of IKKi into IKKn (Fig. 2G, Table S4). A20 inhibition was represented by $kp \times [IKKi] \times (kbA20/(kbA20+[A20] \times TR))$.

Method of module integration and simulation:

To integrate the Base (Table S1) module with either IKK module (Table S3 or Table S4), the intermediate variables pIκBα·NF-κB and pIκBα (Table S2) were combined. The IKK module was the only difference between the integrated models. In Table S7 we display a resulting set of ordinary differential equations for the proposed NF-κB model. In simulations, IκBα and NF-κB molecular species were initialised in their complexed form to the cytoplasmic compartment; all other species were initialised to zero (except for total IKK in the Proposed IKK module which was initialised as IKKn). Models were allowed to equilibrate for 4000-minutes in the absence of TNFα (TR=0). Equilibrium conditions were in agreement with the observed average single cell N:C NF-κB ratio of 0.05 ±0.04 (SD) in the absence of stimulation. The majority of the resting IκBα was complexed with NF-κB but there was a 12% excess, which was in general agreement with existing literature (*21, 28*). For simulation outputs the sum of all NF-κB-containing species was calculated for each compartment independently and normalized to *tv* prior to calculation of the ratio. For the total IκBα, *tv*-normalized compartmental totals were summed.

Reaction	Symbol	Value	References
TNFα stimulation			
TNFα	TR	1/0	on/off (*8*)
Initial concentration per cell			
Total IKK	-	0.08 μM	Initialized as IKKn
IKK parameters			
IKKn → IKKa	*ka*	$0.004s^{-1}$	Fitted, as above
IKKa → IKKi	*ki*	$0.003\ s^{-1}$	Fitted, as above
IKKi → IKKn	***kp***	**$0.0006\ s^{-1}$**	**Fitted**
A20 inhibition rate constant	***kbA20***	**0.0018**	**Fitted, scales *kp* dependent on receptor state *kbA20×TR***
A20 protein synthesis & degradation			
nNF-κB → nNF-κB + tIκBα *Order of hill function, h=2* *Half-max constant, k=0.065^h*	*c1*	$1.4\times10^{-7}\ \mu M^{-1}s^{-1}$	Assumed to be the same as IκBα
tA20→ tA20 + A20	*c2*	$0.5\ s^{-1}$	-
tA20→ Sink	*c3*	$0.00048\ s^{-1}$	Fitted, constrained > tIκBα turnover (Fig. S24)
A20 → Sink	*c4*	**$0.0045\ s^{-1}$**	Fitted

Table S4: Proposed IKK module reactions and parameters.

Parameter scanning, scoring and fitting:

Parameter scans were used to analyse the effects of particular parameter values on model dynamics, and also used as an aid to parameter fitting (Fig. 2F & G, Fig. S8, Fig. S9 and Fig. S10). A function to automate the quantitative scoring of simulated time-series for various TNFα stimulated conditions was constructed in MATLAB 7 (R14).

Scoring Function Simulated outputs (up to 600-minutes) were evaluated based on fitting key characteristics of TNFα stimulation conditions observed in single SK-N-AS:

- ***Continuous TNFα*** Key features were extracted for peaks 3-5 (83% of cells, Fig. 1 and Fig. S2C). Targets: Persistent oscillations with a) troughs no greater than the initial condition (ncNF-κB(0)), b) a period of 100-minutes, and c) a peak nuclear to cytoplasmic ratio of NF-κB equal to 1. (Target values were primarily obtained from SK-N-AS cells transfected with RelA-dsRed and EGFP (*1*)).
- ***Repeat TNFα pulsing*** Key features were extracted for peaks 1-3 (Fig. 2B). Targets: 60- and 100-minute pulse conditions show damping in peak 2 and 3 (target values of 37 and 34% of peak 1 amplitude, Fig. 2B); whereas 200-minute pulse conditions show no damping (see Table S5).

Distances of each the simulation features from experimental targets were scaled to give:

- Scores of a similar order of magnitude, a) between individual feature scores and, b) between each TNFα stimulation condition score (sum of all feature scores within the stimulation condition (e.g. 9 scores for continual, Table S5)).
- A feature score range which reflected experimental observations: A score of 1 was fitted to represent ~1 standard deviation from the mean of the respective feature.

Peaks were classed as a value greater than surrounding time-point values, those below N:C NF-κB of 0.1 were not included based on the lowest experimental measurements.

Troughs were identified from a value lower than surrounding time-points; the first trough that was counted followed the first peak.

Stimulation condition	**Feature**	**Score function** target is lowest score
Continual	Number of peaks	***IF numPeaks > 5*** continue to calculate score ***ELSE*** *total continual score=6*
	Trough: *2*, *3*, *4* (3 scores)	***IF*** *trough> ncNF-κB(0) (trough - ncNF-κB(0))^2 / c* ***ELSE*** *score=0 c=0.0016*
	Peak-peak time: *2:3*, *3:4*, *4:5* (3 scores)	*(period – 100)^2 / c, c=600*
	Peak amplitude: *3*, *4*, *5* (3 scores)	*(amp – 1)^2 / c, c=3*
All repeat pulse	Peak amplitude: *1* (as *ncNF-κB*) (1 score per condition)	*(amp – 4)^2 / c, c=3*
60-min repeat 5-min pulse	Peak amplitude: *2* (as % of *1*)	*(amp – 37)^2 / c, c=600*
	Peak amplitude: *3* (as *ncNF-κB*)	*((amp3 – amp2)^2 / amp2^2) / c, c=0.167*
100-min repeat 5-min pulse	Peak amplitude: *2* (as % of *1*)	*(amp – 34)^2 / c, c=600*
	Peak amplitude: *3* (as *ncNF-κB*)	*((amp3 – amp2)^2 / amp2^2) / c, c=0.167*
200-min repeat 5-min pulse	Peak amplitude: *2* (as % of *1*)	*(amp2 – 100)^2 / c , c=600*
	Peak amplitude: *3* (as % of *1*)	*(amp3 – 100)^2 / c , c=600*

Table S5: Single cell N:C NF-κB time-series features for each TNFα condition

Fitting strategy TNFα stimulations were first fitted for a single 5-minute TNFα pulse, as the most information was available to constrain model parameters for this condition. As single cells showed synchronous behavior with this treatment, bulk cell data (western blot and RT-PCR) were used alongside single cell (N:C NF-κB) to constrain the fit of model parameters. (Any models which did not correctly predict these observations were not considered for scoring of repeat pulse conditions.) Starting with IKK and pIκBα, parameters were fitted manually to total cell IκBα degradation kinetics, then N:C NF-κB amplitude and duration, and mRNA dynamics. The targets for N:C NF-κB fitting of four different TNFα treatment regimes are described in Table S5. Fitting for each condition was repeated in series, and also in reverse order to find the best solution. This included both the deterministic and stochastic models.

Section B: Stochastic 3-feedback NF-κB model: The IκBα-A20-NF-κB model developed herein (Table S1, Table S2 and Table S4) was extended into a stochastic 3-feedback model that in addition to IκBα and A20 loops incorporates delayed feedback due to NF-κB-dependent transcription of IκBε (*9*). Construction of the model incorporated two steps: Firstly, conversion of the 2-loop description from concentrations into number of molecules; secondly, addition of the IκBε feedback loop. Reactions and corresponding parameters considered in the full model are summarized in Table S6. In the model we ignored regulation of the IκBβ isoform since knock-out mouse experiments had shown its limited ability to influence NF-κB temporal kinetics (*9*).

Parameter/Reaction	**Symbol**	**Value**	**Conversion from the deterministic/References**
Spatial parameters			
Total cell volume	*tv*	2700μm^3	-
C:N ratio	*kv*	3.3	-
Conversion parameters			
Number of molecules in 1μm cytoplasmic concentration	*cScale*	1.25×10^6 mol/ μM	Calculated based on the measured cell volume and C:N ratio
Number of molecules in 1μm nuclear concentration	*nScale*	3.8×10^5 mol/ μM	
Initial molecule numbers per cell			
Total NF-κB	-	**100,000**	0.08 μM×cScale
Total IKK	-	**100,000**	0.08 μM×cScale
IKK			
IKKn → IKKa	*ka*	0.004 s^{-1}	-
IKKa → IKKi	*ki*	0.003 s^{-1}	-
IKKi → IKKn	*kp*	0.0006 s^{-1}	-
kbA20	*kbA20*	**3.7×10^3**	0.003 μM×cScale
Complex formation & dissociation			
IκBα + NF-κB → IκBα·NF-κB nIκBα + nNF-κB → nIκBα·nNF-κB	*ka1a* *ka1an*	**4×10^{-7} s^{-1}**	0.5 μM^{-1}s^{-1}/cScale
IκBε + NF-κB → IκBε·NF-κB nIκBε + nNF-κB → nIκBε·nNF-κB	*ka1e* *ka1en*	**4×10^{-7} s^{-1}**	Assumed
IκBα·NF-κB → IκBα + NF-κB nIκBα·nNF-κB → nIκBα + nNF-κB	*kd1a*	5×10^{-4} s^{-1}	-
IκBε·NF-κB → IκBε + NF-κB nIκBε·nNF-κB → nIκBε + nNF-κB	*kd1e*	**5×10^{-4} s^{-1}**	Assumed
NF-κB DNA binding			
nNF-κB+G0→ nNF-κB + G1	*q1*	1.5×10^{-7} s^{-1}	(*29*)
nIκBα +G1→ nIκBα + G0	*q2a*	10^{-6} s^{-1}	(*29*)
nIκBε +G1→ nIκBε + G0	*q2e*	**10^{-6} s^{-1}**	Assumed
Delay in IκBα transcription	T_D	**3600 s**	Fitted
A20 protein synthesis & degradation			
$G1_{A20}$→ tA20	*c1*	**0.0873 s^{-1}**	1.4×10^{-7} μM^{-1}s^{-1}×cScale
tA20→ tA20 + A20	*c2*	0.5 s^{-1}	-
tA20→ Sink	*c3*	0.00048 s^{-1}	-
A20 → Sink	*c4*	0.0045 s^{-1}	-

IκBα protein synthesis & degradation			
$G1_{IκBα}$→ tIκBα	*c1a*	**0.0873 s^{-1}**	1.4×10^{-7} $\mu M^{-1}s^{-1}\times$cScale
tIκBα→ tIκBα + IκBα	*c2a*	0.5 s^{-1}	-
tIκBα→ Sink	*c3a*	0.0003 s^{-1}	-
IκBα→ Sink	*c4a*	0.0005 s^{-1}	-
NF-κB·IκBα→ NF-κB	*c5a*	0.000022 s^{-1}	-
nNF-κB·nIκBα→ nNF-κB	-	0 s^{-1}	-
IKKa + IκBα → pIκBα	*kc1a*	**2.96×10^{-7} s^{-1}**	0.37 $\mu M^{-1}s^{-1}$/cScale
IKKa + IκBα·NF-κB → pIκBα·NF-κB	*kc2a*	**2.96×10^{-7} s^{-1}**	0.37 $\mu M^{-1}s^{-1}$/cScale
pIκBα → Sink	*kt1a*	0.1 s^{-1}	-
pIκBα·NF-κB → Sink	*kt2a*	0.1 s^{-1}	-
IκBε protein synthesis & degradation			
$G1_{IκBε}$→ tIκBε	*c1e*	**0.0291**	Assumed (IκBα/3)
tIκBε→ tIκBε + IκBε	*c2e*	**0.5 s^{-1}**	Assumed
tIκBε→ Sink	*c3e*	**0.0003 s^{-1}**	Assumed
IκBε→ Sink	*c4e*	**0.0005 s^{-1}**	Assumed
NF-κB·IκBε→ NF-κB	*c5e*	**0.000022 s^{-1}**	Assumed
nNF-κB·nIκBε→ nNF-κB	-	**0 s^{-1}**	Assumed
IKKa + IκBε → pIκBε	*kc1e*	**2.96×10^{-7} s^{-1}**	Assumed
IKKa + IκBε·NF-κB → pIκBε·NF-κB	*kc2e*	**2.96×10^{-7} s^{-1}**	Assumed
pIκBε→ Sink	*kt1e*	**0.1 s^{-1}**	Assumed
pIκBε·NF-κB → Sink	*kt2e*	**0.1 s^{-1}**	Assumed
Transport			
NF-κB → nNF-κB	*ki1*	0.0026 s^{-1}	-
nNF-κB → NF-κB	*ke1*	**0.00017 s^{-1}**	0.0026 /50×kv
nIκBα·nNF-κB → IκBα·NF-κB	*ke2a*	**0.033 s^{-1}**	0.01×kv
nIκBε·NF-κB → IκBε·NF-κB	*ke2e*	**0.033 s^{-1}**	Assumed
IκBα → nIκBα	*ki3a*	**0.002 s^{-1}**	0.00067 $s^{-1}\times3$
IκBε → nIκBε	*ki3e*	**0.002 s^{-1}**	Assumed
nIκBα → IκBα	*ke3a*	**0.0099 s^{-1}**	0.000335×kv×3
nIκBε → IκBε	*ke3e*	**0.0099 s^{-1}**	Assumed

Table S6: Construction of the 3-feedback NF-κB model. *Parameters depicted with bold black were converted from concentrations into numbers of molecules. Parameters depicted in red were refitted in the stochastic description. Kinetic parameters/reactions accounting for regulation of IκBε are depicted in blue. Nuclear export rates were adjusted by kv following transition from molar concentrations into number of molecules.*

Model formulation Exact simulation using the well-known stochastic simulation algorithm of Gillespie (*30*) proved to be computationally limited. Instead we utilized a hybrid simulation method that relied on partitioning chemical reactions into *fast* and *slow* ones (*29*). Fast reactions describing evolution of mRNA transcripts and protein molecules were modeled with ODEs (see Table S8), while slow reactions describing regulation of IκBα, IκBε and A20 gene activity were treated as stochastic. We assume that each gene has two homologous copies and can exist in either an *on* or an *off* state, determined by the state of transcription factor binding (*31*). Let $G^i(t)=0,1$, $i=1,2$, denote the binary state of a gene promoter: $G^i=1$ whenever NF-κB is bound to the promoter, and $G^i(t)=0$ otherwise. We assume that transcription of the A20 and IκBα genes is active whenever NF-κB is bound to the promoter and inactive otherwise. We assume the same for the IκBε gene

except that it is assumed that there is a delay of T_D after binding of the NF-κB before the transcription is activated.

For a given transcription factor, the transcription factor binding propensity r^b is the rate at which the transcription factor binds to its unoccupied binding site i.e. if this site is unbound then the probability of binding in a short time interval of duration dt is $r^b dt$. The dissociation propensity r^d is defined similarly. It is assumed that for NF-κB r^b is proportional to the amount of nuclear NF-κB, while the dissociation propensity r^d is proportional to the amount of nuclear IκBα and IκBε, since both IκBs have the ability to inhibit NF-κB DNA binding (*32*). Thus

$$\begin{aligned} r^b(t) &= q_1 \cdot nNF\kappa B(t), \\ r^d(t) &= q_{2a} \cdot nI\kappa B\alpha(t) + q_{2e} \cdot nI\kappa B\varepsilon(t). \end{aligned} \quad (1)$$

The total propensity function *r(t)* for the occurrence of any of the binding or dissociation reaction is given by

$$\begin{aligned} r(t) = {} & r^b_{A20}(t) \cdot (2 - G_{A20}(t)) + r^b_{I\kappa B\alpha}(t) \cdot (2 - G_{I\kappa B\alpha}(t)) + r^b_{I\kappa B\varepsilon}(t) \cdot (2 - G_{I\kappa B\varepsilon}(t)) \\ & + r^d_{A20}(t) \cdot G_{A20}(t) + r^d_{I\kappa B\alpha}(t) \cdot G_{I\kappa B\alpha}(t) + r^d_{I\kappa B\varepsilon}(t) \cdot G_{I\kappa B\varepsilon}(t), \end{aligned} \quad (2)$$

where G_{A20}, $G_{I\kappa B\alpha}$, $G_{I\kappa B\varepsilon}$ denote the ternary state of A20, IκBα and IκBε promoters, respectively.
The stochastic representation of gene activity involves linear regulation, Eq. (1), and it provides a natural saturation for transcription (the deterministic description involves a 2nd-order Hill function).

Simulation algorithm We implemented a numerical scheme for delayed hybrid stochastic stimulations that combines partitioning of the chemical reactions into fast and slow (*29*) and subsequently considering a non-Markovian delay introduced by transcription of IκBε gene (*33*). The algorithm reads:

1. At simulation time t, we calculate the propensity function *r(t)*.
2. We select two random numbers p_1 and p_2 from the uniform distribution on *(0,1)*.
3. Using a fourth-order Matlab solver we evaluate the system of 21 ODEs describing fast reactions, until time $t+\tau$ where τ is such that
$$\log(p_1) + \int_t^{t+\tau} r(s)ds = 0 .$$
Note, that the evaluation the ODE system (Table S8) requires the knowledge of the state of transcriptional activity $G_{I\kappa B\varepsilon}(t-T_D)$ rather than the state of the promoter activity $G_{I\kappa B\varepsilon}(t)$.
4. We determine which reaction j occur at $t+\tau$ by finding the j for which
$$\sum_{i=1}^{j-1} r_i(t+\tau) < p_2 r(t+\tau) \le \sum_{i=1}^{j} r_i(t+\tau),$$
where r_i, $i=1,\ldots,6$ are individual reaction propensities (NF-κB binding/dissociation to/from any of A20, IκBα or IκBε gene promoters).
5. IF delayed reactions are scheduled within *(t, t+τ),* we execute the next delayed reaction at its scheduled time $t+\theta$, and replace t with $t+\theta$,
ELSE
IF j is a delayed reaction then we record the time, $t+\tau+T_D$ for delayed reaction j and we replace t with $t+\tau$,

ELSE we execute reaction *j* and we replace *t* with $t+\tau$.

6. Go back to 1.

Parameters We assumed that kinetic differences between IκBα and IκBε isoforms originated primarily from their transcriptional regulation, rather than their specificity for various NF-κB dimers or the efficiency of IKK mediated degradation (*34-36*). More specifically, we assumed that corresponding IκBα and IκBε kinetic parameters were equal. One notable exception is the delay in IκBε gene transcription and the respective NF-κB dependent transcription rate (Table S6).

While converting the model into a three-feedback model four parameters were changed: the A20 inhibition saturation rate was increased about 2-fold to fit the population dynamics in IκBε knock-out cells. The rate of IKK-dependent phosphorylation of free IκBs was increased 5-fold to reduce the IκBs protein levels in A20 knock-outs *(9)*. We also increased the transport rates of free IκBs by 3-fold to decrease the period of single cell oscillations from 100- to about 80-minutes, which maximizes the IκBε-mediated damping of nuclear NF-κB in a wild-type population of cells.

Model simulations We initialized the system with all NF-κB complexed to IκBs in the cytoplasm, but prior to TNFα stimulation we followed resting single cells for time t uniformly distributed on the interval from 15 to 25 hours. Due to the natural degradation of IκBs and the resulting basal NF-κB translocations sensitivity to any initial conditions was lost.

The stochastic nature of the NF-κB binding and unbinding to the respective promoter implies that a single model simulation is a specific realization of the underlying stochastic process and therefore corresponds to the single-cell level microscopy data. The population kinetics can be captured by the ensemble average. Below, we show the time evolution of the main variables in the system for both the single cells and populations level for continuous stimulations in wild-type, IκBε-/- and A20-/- cells (Fig. S26-Fig. S28) and for repeat TNFα pulsing stimulation in wild-type cells (Fig. S29-Fig. S32).

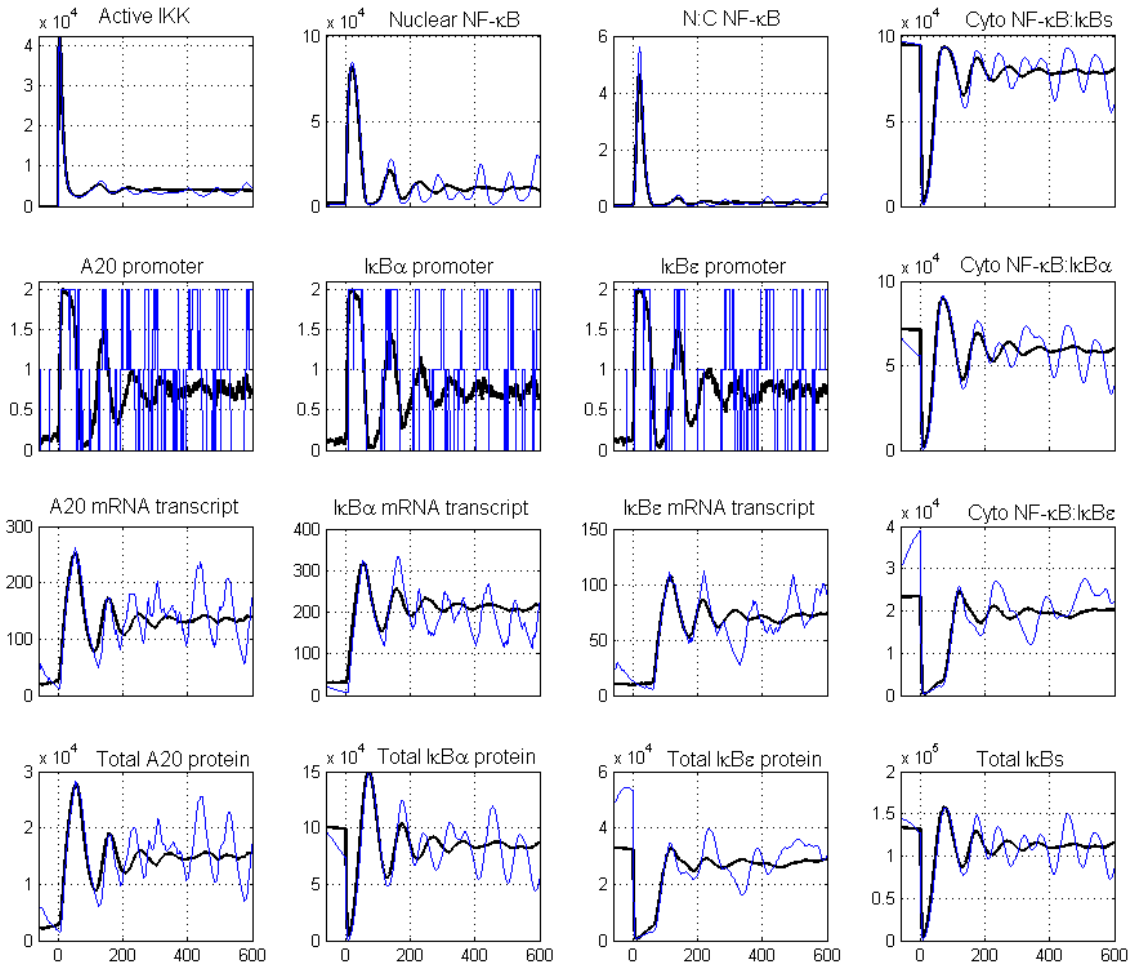

Fig. S26: Time evolution (minutes) of main system variables for wild-type cells. *Population averages based on 100 cells (black line) versus a single cell trajectory (blue line). An expression level of 100,000 NF-κB molecules was assumed. Continuous TNFα treatment was introduced at time t=0 minutes. The individual cell exhibits stimuli-induced stochastic oscillations that are damped at the population level.*

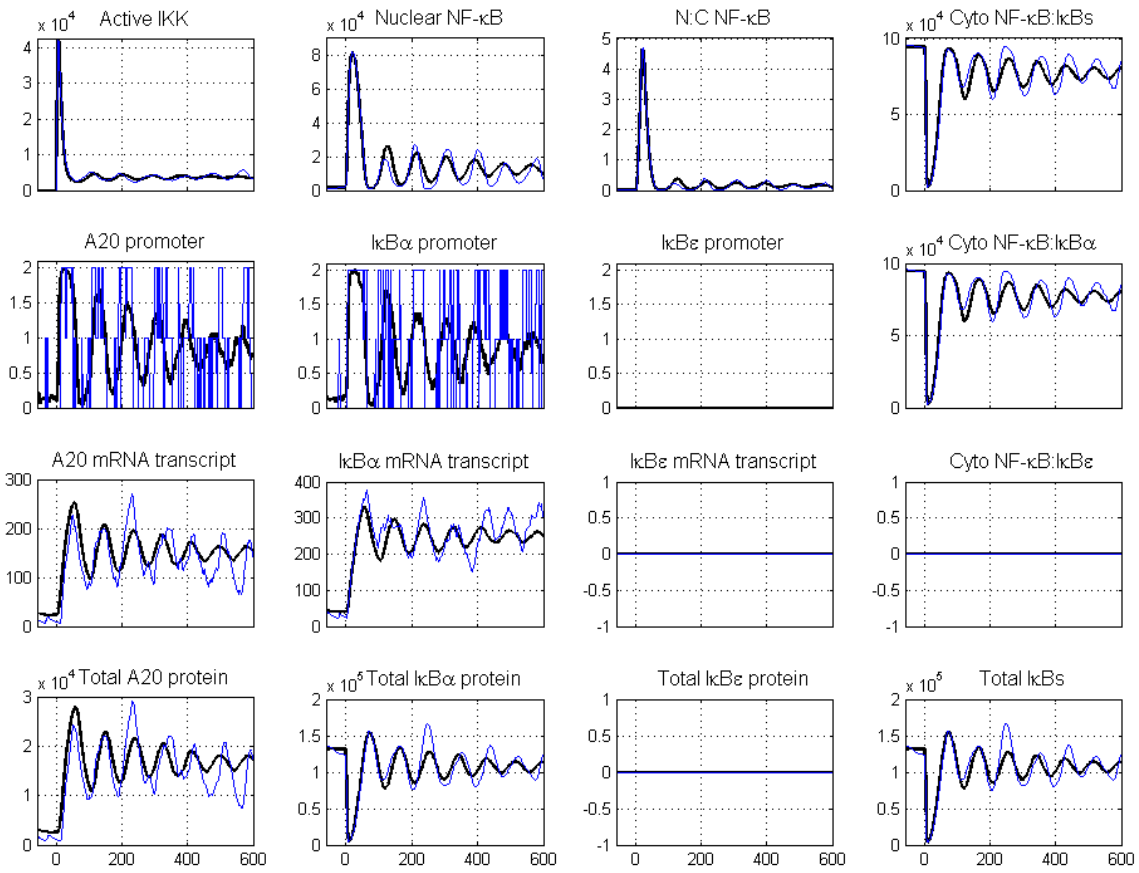

Fig. S27: Time evolution (minutes) of main system variables for the IκBε knock-out. *Population averages based on 100 cells (black line) versus a single cell trajectory (blue line). An expression level of 100,000 NF-κB molecules was assumed. Continuous TNFα treatment was introduced at time t=0 minutes. The individual cells as well as population average exhibited persistent oscillations.*

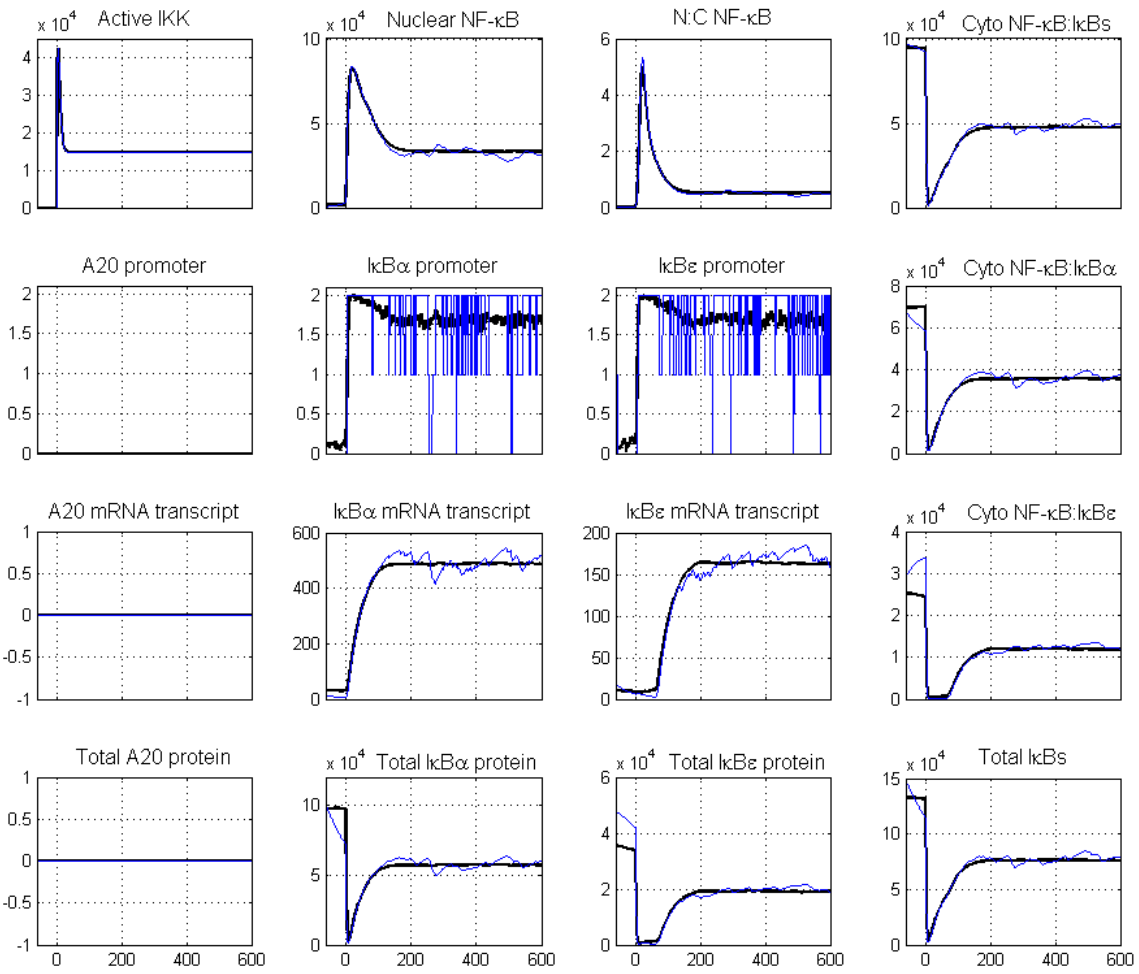

Fig. S28: Time evolution (minutes) of main system variables for the A20 knock-out. *Population averages based on 100 cells (black line) versus a single cell trajectory (blue line). An expression level of 100,000 NF-κB molecules was assumed. Continuous TNFα treatment was introduced at time t=0 minutes.*

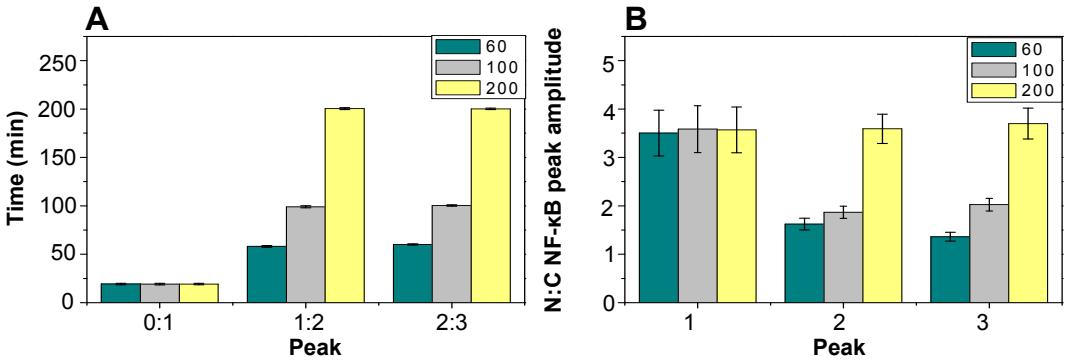

Fig. S29: Analysis of single cell RelA oscillations upon TNFα repeat pulsing. *Population averages (±SD) based on simulated 100 cells. An expression level of 100,000 NF-κB molecules was assumed. (A) Timing between successive peaks. (B) N:C NF-κB amplitude of successive peaks. This should be compared to the data in Fig. 2B.*

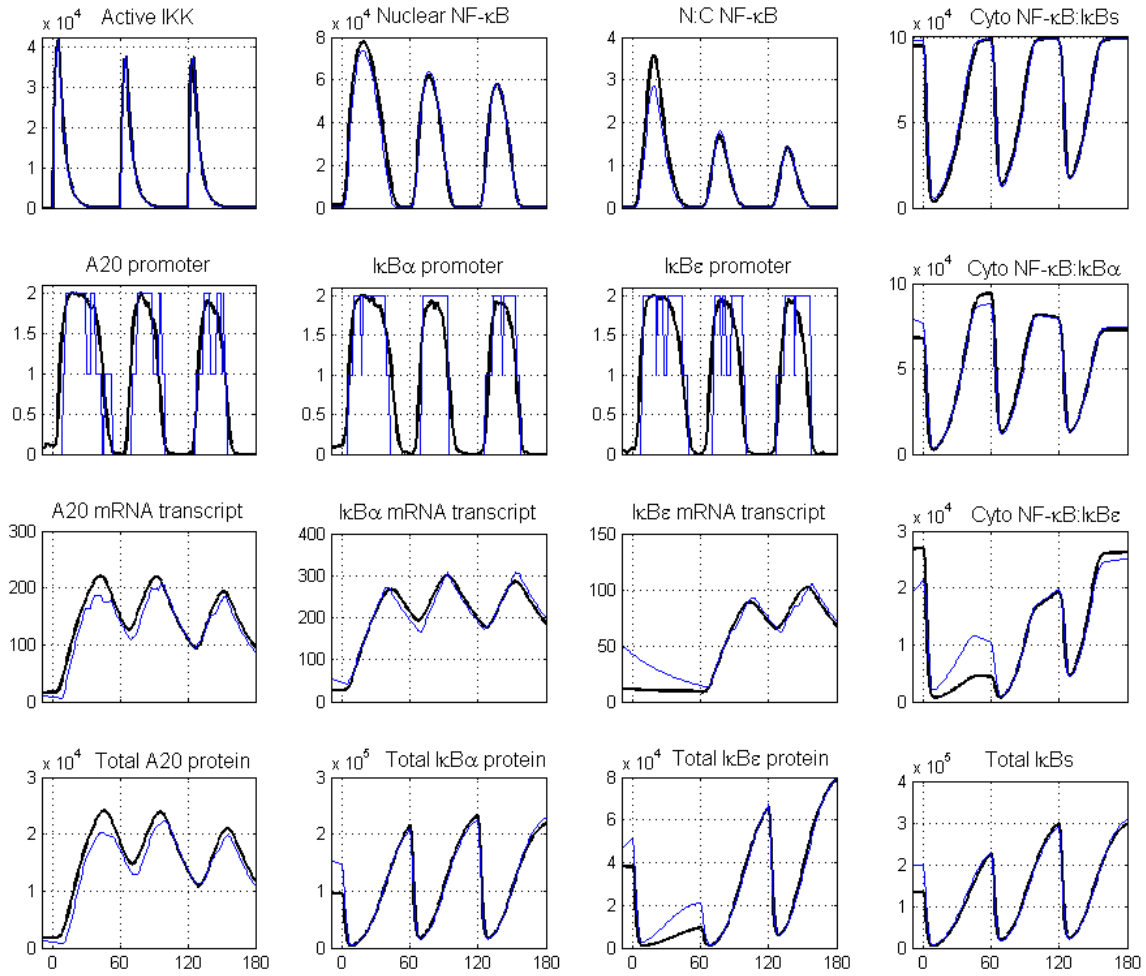

Fig. S30: Time evolution (minutes) of main system variables for the 60-minute repetitive pulsing in wild-type cells. *Population averages based on 100 cells (black line) versus a single cell trajectory (blue line). An expression level of 100,000 NF-κB molecules was assumed. TNFα treatment was introduced at time t=0 minutes.*

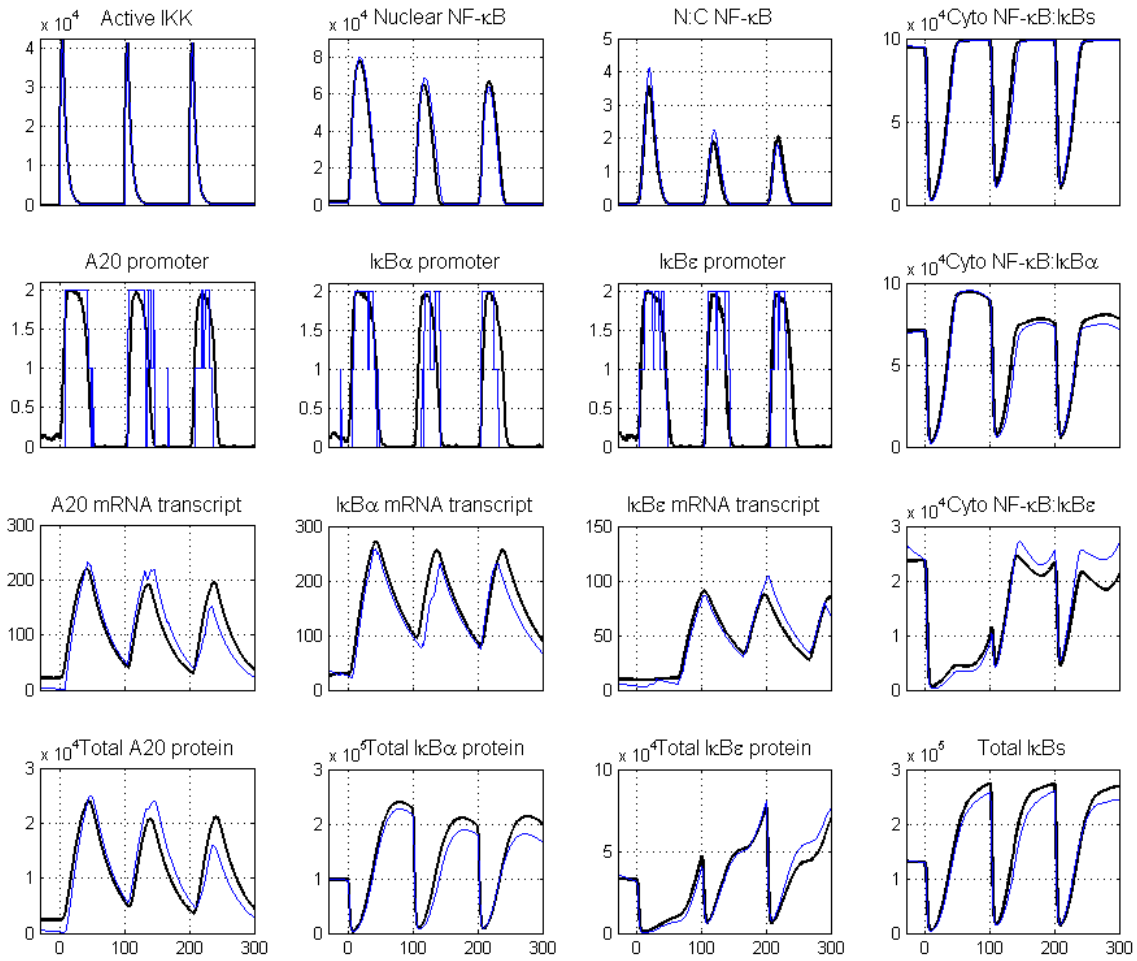

Fig. S31: Time evolution (minutes) of main system variables for the 100-minute repetitive pulsing in wild-type cells. *Population averages based on 100 cells (black line) versus a single cell trajectory (blue line). An expression level of 100,000 NF-κB molecules was assumed. TNFα treatment was introduced at time t=0 minutes.*

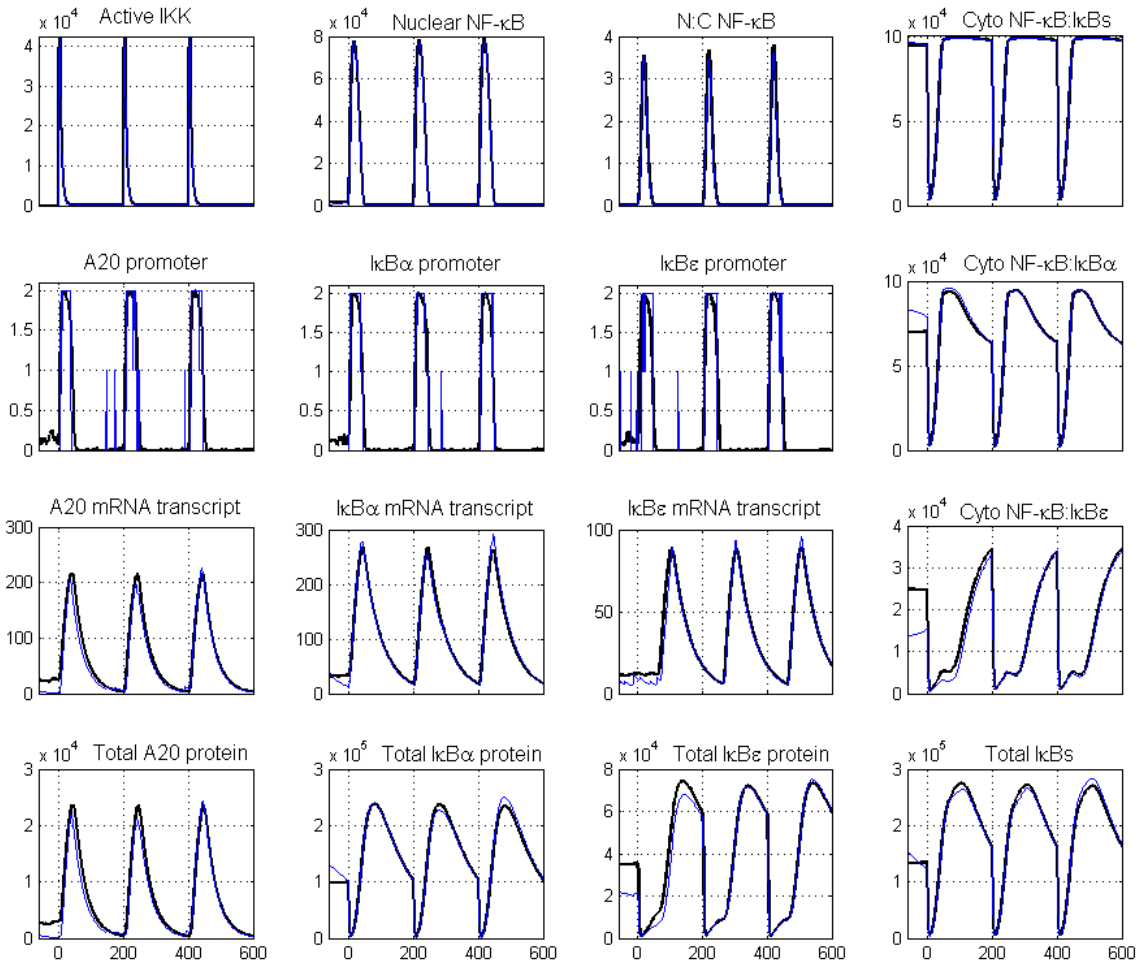

Fig. S32: Time evolution (minutes) of main system variables for the 200-minute repetitive pulsing in wild-type cells. *Population averages based on 100 cells (black line) versus a single cell trajectory (blue line). An expression level of 100,000 NF-κB molecules was assumed. TNFα treatment was introduced at time t=0 minutes.*

Section C: Model equations

Matlab files with equation and simulation routines are available for downloading at http://www.liv.ac.uk/bio/research/groups/cci/.

$$\frac{d}{dt}IKKn(t) = kp \times \frac{kbA20}{kbA20+TR\times A20(t)} \times IKKi(t) - TR \times ka \times IKKn(t) \quad (1)$$

$$\frac{d}{dt}IKKa(t) = TR \times ka \times IKKn(t) - ki \times IKKa(t) \quad (2)$$

$$\frac{d}{dt}IKKi(t) = ki \times IKKa(t) - kp \times \frac{kbA20}{kbA20+TR\times A20(t)} \times IKKi(t) \quad (3)$$

$$\begin{aligned}\frac{d}{dt}NF\kappa B(t) = {} & kd1a \times (I\kappa B\alpha \circ NF\kappa B)(t) - ka1a \times I\kappa B\alpha(t) \times NF\kappa B(t) - ki1 \times NF\kappa B(t) \\ & + ke1 \times nNF\kappa B(t) + kt2a \times (pI\kappa B\alpha \circ NF\kappa B)(t) + c5a \times (I\kappa B\alpha \circ NF\kappa B)(t)\end{aligned} \quad (4)$$

$$\begin{aligned}\frac{d}{dt}nNF\kappa B(t) = {} & kd1a \times (nI\kappa B\alpha \circ nNF\kappa B)(t) - ka1an \times nI\kappa B\alpha(t) \times nNF\kappa B(t) \\ & + ki1 \times kv \times NF\kappa B(t) - ke1 \times kv \times nNF\kappa B(t)\end{aligned} \quad (5)$$

$$\begin{aligned}\frac{d}{dt}I\kappa B\alpha(t) = {} & kd1a \times (I\kappa B\alpha \circ NF\kappa B)(t) - ka1a \times I\kappa B\alpha(t) \times NF\kappa B(t) + c2a \times tI\kappa B\alpha(t) \\ & - c4a \times I\kappa B\alpha(t) - ki3a \times I\kappa B\alpha(t) + ke3a \times nI\kappa B\alpha(t) \\ & - kc1a \times IKKa(t) \times I\kappa B\alpha(t)\end{aligned} \quad (6)$$

$$\begin{aligned}\frac{d}{dt}nI\kappa B\alpha(t) = {} & kd1a \times (nI\kappa B\alpha \circ nNF\kappa B)(t) - ka1an \times nI\kappa B\alpha(t) \times nNF\kappa B(t) \\ & - c4a \times nI\kappa B\alpha(t) + ki3a \times kv \times I\kappa B\alpha(t) - ke3a \times kv \times nI\kappa B\alpha(t)\end{aligned} \quad (7)$$

$$\frac{d}{dt}A20(t) = c2 \times tA20(t) - c4 \times A20(t) \quad (8)$$

$$\frac{d}{dt}tI\kappa B\alpha(t) = c1a \times \frac{nNF\kappa B^h(t)}{nNF\kappa B^h(t)+k^h} - c3a \times tI\kappa B\alpha(t) \quad (9)$$

$$\frac{d}{dt}tA20(t) = c1 \times \frac{nNF\kappa B^h(t)}{nNF\kappa B^h(t)+k^h} - c_3 \times tA20(t) \quad (10)$$

$$\frac{d}{dt}pI\kappa B\alpha(t) = kc1a \times IKKa(t) \times I\kappa B\alpha(t) - kt1a \times pI\kappa B\alpha(t) \quad (11)$$

$$\frac{d}{dt}(pI\kappa B\alpha \circ NF\kappa B)(t) = kc2a \times IKKa(t) \times (I\kappa B\alpha \circ NF\kappa B)(t) - kt2a \times (pI\kappa B\alpha \circ NF\kappa B)(t) \quad (12)$$

$$\begin{aligned}\frac{d}{dt}(I\kappa B\alpha \circ NF\kappa B)(t) = {} & ka1a \times I\kappa B\alpha(t) \times NF\kappa B(t) - kd1a \times (I\kappa B\alpha \circ NF\kappa B)(t) \\ & - c5a \times (I\kappa B\alpha \circ NF\kappa B)(t) + ke2a \times (nI\kappa B\alpha \circ nNF\kappa B)(t) \\ & - kc2a \times IKKa(t) \times (I\kappa B\alpha \circ NF\kappa B)(t)\end{aligned} \quad (13)$$

$$\begin{aligned}\frac{d}{dt}(nI\kappa B\alpha \circ nNF\kappa B)(t) = {} & ka1an \times nI\kappa B\alpha(t) \times nNF\kappa B(t) - kd1a \times (nI\kappa B\alpha \circ nNF\kappa B)(t) \\ & - ke2a \times kv \times (nI\kappa B\alpha \circ nNF\kappa B)(t)\end{aligned} \quad (14)$$

Table S7. Differential equations for the 2-feedback NF-κB model. Equations describe reactions included in Table S1, Table S2 and Table S4. All the substrates were quantified by their molar concentrations. Symbol *n* denotes nuclear variables, *t* denotes mRNA transcript, while *p* denotes phosphorylated form of IκBα. Symbols denoting cytoplasmic localization were omitted. Transport rates for nuclear variables (Eqs. (5), (6) and (14)) were adjusted by k_v (ratio of cytoplasmic and nuclear volume) to reflect smaller nuclear volume; hence increasing molecular concentrations within this compartment.

$$\frac{d}{dt} IKKn(t) = kp \times \frac{kbA20}{kbA20 + TR \times A20(t)} \times IKKi(t) - TR \times ka \times IKKn(t) \quad (1)$$

$$\frac{d}{dt} IKKa(t) = TR \times ka \times IKKn(t) - ki \times IKKa(t) \quad (2)$$

$$\frac{d}{dt} IKKi(t) = ki \times IKKa(t) - kp \times \frac{kbA20}{kbA20 + TR \times A20(t)} \times IKKi(t) \quad (3)$$

$$\begin{aligned} \frac{d}{dt} NF\kappa B(t) = {} & kd1a \times \left(I\kappa B\alpha \circ NF\kappa B\right)(t) + kd1e \times \left(I\kappa B\varepsilon \circ NF\kappa B\right)(t) \\ & - ka1a \times I\kappa B\alpha(t) \times NF\kappa B(t) - ka1e \times I\kappa B\varepsilon(t) \times NF\kappa B(t) - ki1 \times NF\kappa B(t) \\ & + ke1 \times nNF\kappa B(t) + kt2a \times \left(pI\kappa B\alpha \circ NF\kappa B\right)(t) + kt2e \times \left(pI\kappa B\varepsilon \circ NF\kappa B\right)(t) \\ & + c5a \times \left(I\kappa B\alpha \circ NF\kappa B\right)(t) + c5e \times \left(I\kappa B\varepsilon \circ NF\kappa B\right)(t) \end{aligned} \quad (4)$$

$$\begin{aligned} \frac{d}{dt} nNF\kappa B(t) = {} & kd1a \times \left(nI\kappa B\alpha \circ nNF\kappa B\right)(t) + kd1e \times \left(nI\kappa B\varepsilon \circ nNF\kappa B\right)(t) \\ & - ka1an \times kv \times nI\kappa B\alpha(t) \times nNF\kappa B(t) - ka1en \times kv \times nI\kappa B\varepsilon(t) \times nNF\kappa B(t) \\ & + ki1 \times NF\kappa B(t) - ke1 \times nNF\kappa B(t) \end{aligned} \quad (5)$$

$$\begin{aligned} \frac{d}{dt} I\kappa B\alpha(t) = {} & kd1a \times \left(I\kappa B\alpha \circ NF\kappa B\right)(t) - ka1a \times I\kappa B\alpha(t) \times NF\kappa B(t) + c2a \times tI\kappa B\alpha(t) \\ & - c4a \times I\kappa B\alpha(t) - ki3a \times I\kappa B\alpha(t) + ke3a \times nI\kappa B\alpha(t) \\ & - kc1a \times IKKa(t) \times I\kappa B\alpha(t) \end{aligned} \quad (6)$$

$$\begin{aligned} \frac{d}{dt} I\kappa B\varepsilon(t) = {} & kd1e \times \left(I\kappa B\varepsilon \circ NF\kappa B\right)(t) - ka1e \times I\kappa B\varepsilon(t) \times NF\kappa B(t) + c2e \times tI\kappa B\varepsilon(t) \\ & - c4e \times I\kappa B\varepsilon(t) - ki3e \times I\kappa B\varepsilon(t) + ke3e \times nI\kappa B\alpha(t) \\ & - kc1e \times IKKa(t) \times I\kappa B\varepsilon(t) \end{aligned} \quad (7)$$

$$\begin{aligned} \frac{d}{dt} nI\kappa B\alpha(t) = {} & kd1a \times \left(nI\kappa B\alpha \circ nNF\kappa B\right)(t) - ka1an \times kv \times nI\kappa B\alpha(t) \times nNF\kappa B(t) \\ & - c4a \times nI\kappa B\alpha(t) + ki3a \times I\kappa B\alpha(t) - ke3a \times nI\kappa B\alpha(t) \end{aligned} \quad (8)$$

$$\begin{aligned} \frac{d}{dt} nI\kappa B\varepsilon(t) = {} & kd1e \times \left(nI\kappa B\varepsilon \circ nNF\kappa B\right)(t) - ka1en \times kv \times nI\kappa B\varepsilon(t) \times nNF\kappa B(t) \\ & - c4e \times nI\kappa B\varepsilon(t) + ki3e \times I\kappa B\varepsilon(t) - ke3e \times nI\kappa B\varepsilon(t) \end{aligned} \quad (9)$$

$$\frac{d}{dt} A20(t) = c2 \times tA20(t) - c4 \times A20(t) \quad (11)$$

$$\frac{d}{dt} tI\kappa B\alpha(t) = c1a \times G_{I\kappa B\alpha}(t) - c3a \times tI\kappa B\alpha(t) \quad (12)$$

$$\frac{d}{dt} tI\kappa B\varepsilon(t) = c1e \times G_{I\kappa B\varepsilon}(t - T_D) - c3e \times tI\kappa B\varepsilon(t) \quad (13)$$

$$\frac{d}{dt} tA20(t) = c1 \times G_{A20}(t) - c3 \times tA20(t) \quad (14)$$

$$\frac{d}{dt} pI\kappa B\alpha(t) = kc1a \times IKKa(t) \times I\kappa B\alpha(t) - kt1a \times pI\kappa B\alpha(t) \quad (15)$$

$$\frac{d}{dt} pI\kappa B\varepsilon(t) = kc1e \times IKKa(t) \times I\kappa B\varepsilon(t) - kt1e \times pI\kappa B\varepsilon(t) \quad (16)$$

$$\frac{d}{dt} \left(pI\kappa B\alpha \circ NF\kappa B\right)(t) = kc2a \times IKKa(t) \times \left(I\kappa B\alpha \circ NF\kappa B\right)(t) - kt2a \times \left(pI\kappa B\alpha \circ NF\kappa B\right)(t) \quad (17)$$

$$\frac{d}{dt} \left(pI\kappa B\varepsilon \circ NF\kappa B\right)(t) = kc2e \times IKKa(t) \times \left(I\kappa B\varepsilon \circ NF\kappa B\right)(t) - kt2e \times \left(pI\kappa B\varepsilon \circ NF\kappa B\right)(t) \quad (18)$$

$$\begin{aligned} \frac{d}{dt} \left(I\kappa B\alpha \circ NF\kappa B\right)(t) = {} & ka1a \times I\kappa B\alpha(t) \times NF\kappa B(t) - kd1a \times \left(I\kappa B\alpha \circ NF\kappa B\right)(t) \\ & - c5a \times \left(I\kappa B\alpha \circ NF\kappa B\right)(t) + ke2a \times \left(nI\kappa B\alpha \circ nNF\kappa B\right)(t) \\ & - kc2a \times IKKa(t) \times \left(I\kappa B\alpha \circ NF\kappa B\right)(t) \end{aligned} \quad (19)$$

$$\begin{aligned} \frac{d}{dt} \left(I\kappa B\varepsilon \circ NF\kappa B\right)(t) = {} & ka1e \times I\kappa B\varepsilon(t) \times NF\kappa B(t) - kd1e \times \left(I\kappa B\varepsilon \circ NF\kappa B\right)(t) \\ & - c5e \times \left(I\kappa B\varepsilon \circ NF\kappa B\right)(t) + ke2e \times \left(nI\kappa B\varepsilon \circ nNF\kappa B\right)(t) \\ & - kc2e \times IKKa(t) \times \left(I\kappa B\varepsilon \circ NF\kappa B\right)(t) \end{aligned} \quad (20)$$

$$\frac{d}{dt}\left(nI\kappa B\alpha \circ nNF\kappa B\right)(t) = ka1an \times kv \times nI\kappa B\alpha(t) \times nNF\kappa B(t) - kd1a \times \left(nI\kappa B\alpha \circ nNF\kappa B\right)(t) - ke2a \times \left(nI\kappa B\alpha \circ nNF\kappa B\right)(t) \quad (21)$$

$$\frac{d}{dt}\left(nI\kappa B\varepsilon \circ nNF\kappa B\right)(t) = ka1en \times kv \times nI\kappa B\varepsilon(t) \times nNF\kappa B(t) - kd1e \times \left(nI\kappa B\varepsilon \circ nNF\kappa B\right)(t) - ke2e \times \left(nI\kappa B\varepsilon \circ nNF\kappa B\right)(t) \quad (22)$$

Table S8. Differential equations describing deterministic part of the 3-feedback NF-κB model. All the substrates were quantified by the number of molecules. Symbol *n* denotes nuclear variables, *t* denotes mRNA transcript, while *p* denotes phosphorylated form of IκBα and IκBε. Symbols denoting cytoplasmic localization were omitted. Nuclear association rates (Eqs. (5), (6), (9), (21) and (22)) were adjusted by k_v to reflect transition from concentrations into number of molecules. For nuclear export rates also changed by the transformation, we adjusted parameter values (Table S6) rather than equations.

3. Statement of author contributions:

Louise Ashall performed and designed the ChIP, qPCR and siRNA studies and helped to write the manuscript. Caroline Horton developed the deterministic model, performed a considerable amount of data analysis and integration and helped to write the manuscript. David Nelson initiated the repeated TNFα pulse work and performed the imaging work and western blotting in Fig. 2 and the semi-quantitative PCR that led to Fig. 4. Pawel Paszek developed the stochastic model, designed the siRNA experiment in Fig. 3 and helped to write the manuscript. Claire Harper constructed and analyzed the SK-N-AS stable cell line and assisted with the planning of the qPCR experiments. Kate Sillitoe performed the experiments to study oscillations in mouse embryonic fibroblasts. Sheila Ryan assisted with the ChIP and qPCR assays. Dave Spiller runs the microscopes in the Centre for Cell Imaging and assisted with microscopy experiment design and subsequent analysis. John Unitt was the joint supervisor for Kate Sillitoe's work and advised on the project. Dave Broomhead assisted Caroline Horton with the development of the deterministic model. Douglas Kell assisted with the deterministic modeling work and data interpretation and commented on the manuscript. David Rand advised Caroline Horton with the scoring and interpretation of the models and commented on the manuscript. Violaine Sée assisted with the design and interpretation of the ChIP and siRNA experiments and assisted with qPCR assays. Michael White directed the project and wrote the manuscript.

4. Supplementary references

1. D. E. Nelson *et al.*, *Science* **306**, 704 (Oct 22, 2004).
2. G. Rabut, J. Ellenberg, *J Microsc* **216**, 131 (Nov, 2004).
3. H. Shen *et al.*, *J R Soc Interface* **3**, 787 (Dec 22, 2006).
4. D. Bosisio *et al.*, *Embo J* **25**, 798 (Feb 22, 2006).
5. J. Iqbal, M. Zaidi, *Biochem Biophys Res Commun* **371**, 906 (Jul 11, 2008).
6. L. Sun, G. Yang, M. Zaidi, J. Iqbal, *Biochem Biophys Res Commun* **371**, 900 (Jul 11, 2008).
7. L. Sun, G. Yang, M. Zaidi, J. Iqbal, *Biochem Biophys Res Commun* **371**, 912 (Jul 11, 2008).
8. T. Lipniacki, P. Paszek, A. R. Brasier, B. Luxon, M. Kimmel, *J Theor Biol* **228**, 195 (May 21, 2004).
9. J. D. Kearns, S. Basak, S. L. Werner, C. S. Huang, A. Hoffmann, *J Cell Biol* **173**, 659 (Jun 5, 2006).
10. D. E. Nelson *et al.*, *Science* **308** (Apr 1, 2005).
11. R. Cheong *et al.*, *J Biol Chem* **281**, 2945 (Feb 3, 2006).
12. E. L. O'Dea *et al.*, *Mol Syst Biol* **3**, 111 (2007).
13. S. L. Werner, D. Barken, A. Hoffmann, *Science* **309**, 1857 (Sep 16, 2005).
14. E. G. Lee *et al.*, *Science* **289**, 2350 (Sep 29, 2000).
15. R. Cheong, A. Hoffmann, A. Levchenko, *Mol Syst Biol* **4**, 192 (2008).
16. A. Hoffmann, A. Levchenko, M. L. Scott, D. Baltimore, *Science* **298**, 1241 (Nov 8, 2002).
17. A. M. Femino, F. S. Fay, K. Fogarty, R. H. Singer, *Science* **280**, 585 (Apr 24, 1998).
18. C. Blattner *et al.*, *Mol Cell Biol* **20**, 3616 (May, 2000).
19. E. Mathes, E. L. O'Dea, A. Hoffmann, G. Ghosh, *Embo J* **27**, 1357 (May 7, 2008).
20. M. P. Pando, I. M. Verma, *J Biol Chem* **275**, 21278 (Jul 14, 2000).
21. F. Carlotti, S. K. Dower, E. E. Qwarnstrom, *J Biol Chem* **275**, 41028 (Dec 29, 2000).
22. C. Y. Ito, A. G. Kazantsev, A. S. Baldwin, Jr., *Nucleic Acids Res* **22**, 3787 (Sep 11, 1994).
23. A. Krikos, C. D. Laherty, V. M. Dixit, *J Biol Chem* **267**, 17971 (Sep 5, 1992).
24. R. Heilker, F. Freuler, R. Pulfer, F. Di Padova, J. Eder, *Eur J Biochem* **259**, 253 (Jan, 1999).
25. E. Zandi, M. Karin, *Mol Cell Biol* **19**, 4547 (Jul, 1999).
26. G. Nelson *et al.*, *J Cell Sci* **115**, 1137 (Mar 15, 2002).
27. H. Hacker, M. Karin, *Sci STKE* **2006**, re13 (Oct 17, 2006).
28. N. R. Rice, M. K. Ernst, *Embo J* **12**, 4685 (Dec, 1993).
29. T. Lipniacki, P. Paszek, A. R. Brasier, B. A. Luxon, M. Kimmel, *Biophys J* **90**, 725 (Feb 1, 2006).
30. D. T. Gillespie, *J. Phys. Chem* **81**, 2340 (1977).
31. J. M. Raser, E. K. O'Shea, *Science* **304**, 1811 (Jun 18, 2004).
32. S. H. Lee, M. Hannink, *J Biol Chem* **277**, 23358 (Jun 28, 2002).
33. M. Barrio, K. Burrage, A. Leier, T. Tian, *PLoS Comput Biol* **2**, e117 (Sep 8, 2006).

34. S. Doerre *et al.*, *J Immunol* **174**, 983 (Jan 15, 2005).
35. M. Spiecker, H. Darius, J. K. Liao, *J Immunol* **164**, 3316 (Mar 15, 2000).
36. S. T. Whiteside, J. C. Epinat, N. R. Rice, A. Israel, *Embo J* **16**, 1413 (Mar 17, 1997).